TECHNICAL REPORT ARLCD-TR-77065

CHARCOAL REGENERATION

PART I

MECHANISM OF TNT ADSORPTION

THOMAS C. CASTORINA
JEROME HABERMAN
JAGADISH SHARMA

NOVEMBER 1977

US ARMY ARMAMENT RESEARCH AND DEVELOPMENT COMMAND
LARGE CALIBER
WEAPON SYSTEMS LABORATORY
DOVER, NEW JERSEY

UNCLASSIFIED

SECURITY CLASSIFICATION OF THIS PAGE (When Data Entered)

REPORT DOCUMENTATION PAGE

READ INSTRUCTIONS BEFORE COMPLETING FORM

1. REPORT NUMBER: Technical Report ARLCD-TR-77065
2. GOVT ACCESSION NO.
3. RECIPIENT'S CATALOG NUMBER
4. TITLE (and Subtitle): CHARCOAL REGENERATION, PART I. MECHANISM OF TNT ADSORPTION.
5. TYPE OF REPORT & PERIOD COVERED
6. PERFORMING ORG. REPORT NUMBER
7. AUTHOR(s): Thomas C. Castorina, Jerome Haberman and Jagadish Sharma
8. CONTRACT OR GRANT NUMBER(s): 3627-01-001
9. PERFORMING ORGANIZATION NAME AND ADDRESS: Large Caliber Weapons Systems Laboratory, US Army Armament Research and Development Command, Dover, New Jersey 07801
10. PROGRAM ELEMENT, PROJECT, TASK AREA & WORK UNIT NUMBERS: 1L762720D048S-10
11. CONTROLLING OFFICE NAME AND ADDRESS: Chemical Systems Laboratory, ARRADCOM CLT - P, Aberdeen Proving Ground, MD 21010
12. REPORT DATE: November 1977
13. NUMBER OF PAGES: 53
14. MONITORING AGENCY NAME & ADDRESS (if different from Controlling Office): 52p.
15. SECURITY CLASS. (of this report): Unclassified
15a. DECLASSIFICATION/DOWNGRADING SCHEDULE
16. DISTRIBUTION STATEMENT (of this Report): Approved for public release, distribution unlimited.
18. SBIE; 19. AD-E400 023

17. DISTRIBUTION STATEMENT (of the abstract entered in Block 20, if different from Report)
18. SUPPLEMENTARY NOTES
19. KEY WORDS (Continue on reverse side if necessary and identify by block number)

Activated carbon
Physical and chemical adsorption
Carbon wastewater treatment
Deactivation of carbon surface
TNT interaction with charcoal surface

20. ABSTRACT (Continue on reverse side if necessary and identify by block number)

The interaction of TNT with the surface of activated carbon (FS300) has been studied via adsorption isotherms of TNT and water, surface area determinations and electron spectroscopy for chemical analysis (ESCA). The rate and extent of adsorption of TNT is strongly dependent on the particle size of FS300 and hence on the diffusion rate, and independent of pH and temperature. The process of deactivation of the carbon surface is shown to involve progressive irreversible occlusion of the microporous structure with each

DD FORM 1 JAN 73 1473 EDITION OF 1 NOV 65 IS OBSOLETE

UNCLASSIFIED

SECURITY CLASSIFICATION OF THIS PAGE (When Data Entered)

410 163

20. ABSTRACT (Contd)

successive adsorption/desorption (with acetone) cycle. The irreversibility of TNT adsorption is attributed to chemical interaction and a mechanism for the deactivation of the carbon surface is postulated.

The citation in this report of the names of commercial firms or commercially available products or services does not constitute official endorsement or approval of such commercial firms, products, or services by the U. S. Government.

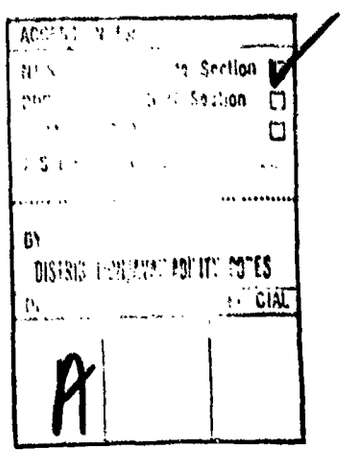

ACKNOWLEDGEMENT

Professor F.J. Micale of Lehigh University, Bethlehem, PA, is especially cited for the significant contributions he made under contract DAAG29-76-D-0100 on the water adsorption measurements and the many helpful discussions dealing with the more fundamental aspects of the surface characteristics of activated carbon.

This study was funded under the Environmental Quality R&D program administered by the DARCOM Lead Laboratory for PAECT, Aberdeen Proving Ground, MD.

TABLE OF CONTENTS

INTRODUCTION

Carbon adsorption treatment of pink wastewater (TNT/RDX) is being used at the Load-Assembly-Packaging Division of Joliet, Iowa, Kansas and Toole Army Ammunition Plants. Presently the method of disposing of the TNT/RDX saturated carbon is by incineration which is costly and presents a potential for air pollution. Alternative methods of handling the pink wastewater problem are currently under investigation. Iowa Army Ammunition Plant (IAAP) is studying thermal regeneration of carbon, and Natick Laboratories polymer resin adsorption. The economics of both methods are being evaluated for a decision on adoption. A method having the adsorptive capacity of carbon which could be regenerated on column without disassembly by elution techniques would be the ideal solution. This latter approach is the basis of the study being conducted at ARRADCOM. Since TNT replaces RDX from the adsorbed state and TNT remains strongly bound to the carbon surface (Ref 1), the study of the process of carbon degeneration was initially restricted to TNT. The first phase of this study which deals with the determination of the mechanism by which TNT is adsorbed on carbon is the subject of this report.

EXPERIMENTAL

FS300 Charcoal

The activated charcoal used in this study was obtained from Calgon Corporation, Pittsburg, PA. It is prepared from bituminous coal, having a pore size distribution, by volume, of 0.438 cc/g of micropore diameters 5-15A, 0.172 cc/g of transitional (meso) pore diameters 15-200A and 0.215 cc/g of macropore diameters >200A. The surface area of random samples taken from the master batch, as determined by the Brunauer, Emmett and Teller (BET) method, is 1050 $M^2/g \pm 35\ M^2/g$ which compares favorably with the value reported by the supplier, viz, 1000 M^2/g.

Preparation of Various Particle Sizes of FS300

FS300 was ground in a mortar and pestle and passed through a series of US standard sieves. The ground charcoal passing through a 325 sieve (average particle diameter, 44 microns) was designated as fine particle size FS300. Medium particle size FS300 was retained on a 80 sieve (average particle diameter of 300 microns) after passing through a 40 sieve. Coarse FS300 was the unground charcoal as received from the supplier (average particle diameter of 850 microns) termed "as is". All batches of FS300 were washed with distilled water by decantation to remove fines, and then dried in an oven at 150°C. The surface areas of all three particle sizes were the same within experimental error: coarse = 1098 M^2/g, medium = 1069 M^2/g and fine = 1055 M^2/g.

Ultraviolet Analysis of Aqueous Solutions

A Beckman DK recording spectrophotometer equipped with one centimeter pathlength matched quartz cells was used for the analysis of aqueous solutions of TNT. A stock solution of TNT (100 ppm) was prepared by dissolving 100 mg of recrystallized TNT in one liter of doubly distilled water. Aliquots of stock solution were taken to prepare 1 to 10 ppm inclusively of standard TNT solutions. The absorbances of these standard solutions were read on the spectrophotometer at 230 nm against a water blank. The absorbances were plotted vs concentration and the 1 to 10 ppm plot was observed to be linear. For convenience, the slope of the line was calculated. Unknown solutions to be analyzed were diluted to a concentration in the range of 1 to 10 ppm. Their respective absorbances were multiplied by the slope and the appropriate dilution factor applied to give the concentration of TNT in parts per million. The accuracy of the method is illustrated in Table 1.

Adsorption-Desorption Determinations

For the adsorption determinations a constant weight of FS300 to volume of TNT stock solution was maintained. This ratio assured adsorption at the plateau region of the adsorption isotherms at equilibrium. To a one liter glass-stoppered Erlenmeyer flask was added 100 mg of FS300 and 500 ml of aqueous TNT solution (~130 ppm). The charged flask was placed on a wrist-action shaker and shaken for a minimum of 48 hours to assure saturation of the charcoal. The amount adsorbed by the charcoal was determined by withdrawing an aliquot of supernatant solution from the flask, diluting with water to give a concentration of TNT between 1 to 10 ppm, and measuring the concentration of ultraviolet (UV) analysis. This measured concentration, C_1, was subtracted from the initial concentration, C_o of TNT solution in ppm and the specific adsorption calculated by equation 1:

$$\text{Specific adsorption} = \frac{C_o - C_1}{2m} \qquad (1)$$

where m = weight of charcoal
2 = correction factor for the volume of TNT solution used in the adsorption determination

After having performed the adsorption determination, the TNT-saturated charcoal was prepared for the desorption of TNT by decanting the TNT solution from the flask and rinsing the retained charcoal once with a small amount of water. After adding 50 ml of C.P.

acetone, the flask was stoppered and placed on the shaker and shaken overnight. The acetone was decanted into a beaker, followed by a wash of the charcoal with a minimum of acetone. The desorption procedure was carried out two more times by shaking each time for one hour with 50 ml of acetone. All washings were transferred to a 250 ml volumetric flask and diluted to mark. A 5 ml aliquot was pipetted into a 250 ml beaker containing 40 ml of distilled water. The solution was brought to a gentle boil on a hot plate and concentrated to a final volume of 10 to 15 ml. By this process the acetone was expelled yielding a residual aqueous solution of TNT which was diluted to volume (100 ml) and the concentration, C, determined as described in this section. Known amounts of TNT in acetone were subjected to the same treatment with 100% recovery.

The specific desorption (sp. des.) of TNT was calculated according to equation 2:

$$\text{Sp.des. of TNT} = 50 \times \frac{100}{1000} \times \frac{C}{M} = 5 \times \frac{C}{M} \qquad (2)$$

where M = weight of charcoal
C = concentration of TNT, ppm

Surface Area Measurement

A BET type adsorption apparatus, equipped with stainless steel bellows valves was used to measure the surface area of FS300 charcoal with argon at -196°C. Pressures were read with a Baratron micromanometer having a sensitivity of 0.01 torr. Six replicate surface area determinations of a charcoal sample had a standard deviation of 1050 ± 35 M^2/g.

Gas Chromatographic Analysis

A Varian Aerograph Model 1868 gas chromatograph (GC), equipped with a flame ionization detector, and a 3 M x 0.63 cm stainless steel column packed with 4% Dexil on ABS support, was used for the analysis of the acetone eluent of TNT-saturated charcoal. Five microliter aliquots of the acetone solutions were chromatographed with programing from 100°C to 225°C at a rate of 8°C per minute.

Infrared Analysis

A Perkin Elmer 457A Grating Infrared (IR) Spectrophotometer was employed for the analysis of the strongly adsorbed TNT charcoal

adduct. Approximately 1 mg of the sample was pelleted with KBr and the spectrum compared with a standard of pure TNT.

Water Adsorption Isotherms

The water adsorptions were measured gravimetrically on a quartz spring balance (Worden Quartz Products, Inc.) which had an absolute sensitivity of 0.2 microgram and a relative sensitivity of 7 microgram per gram of sample. The water vapor pressures were measured with a 100 mm Barocol (Datametrics, Inc.) capacitive differential manometer sensor and associated electronics enabling accurate readings to better than 10^{-3} mm.

Electrophoretic Mobility Measurements

The electrophoretic mobility measurements were obtained by means of a capillary electrophoresis apparatus (Rank Brothers, Ltd.) with an accuracy of ± 0.1 μm/volt sec. The charcoal samples in every case were crushed manually in a mortar and pestle and dispersed ultrasonically in order to obtain a dispersion suitable for measurement.

Mass Spectrometric Analysis

A DuPont Model 492 high resolution mass spectrometer (MS) was used to analyze the strongly adsorbed TNT adduct on charcoal. The sample was inserted in a 3 cm length capillary tube. After stripping off the residual acetone, the capillary containing the solid residue was introduced into the source by means of the solid probe. The source chamber was heated to 125°C and the mass spectral analysis run in the electron impact mode. The spectrum was scanned up to 400 atomic mass units (amu).

Electron Spectroscopic Analysis

The electron spectroscopic analysis (ESCA) of TNT/charcoal samples and various acetone extracts was carried out using a Varian I.E.E. -15 photoelectron spectrometer with a Mg anode for the production of characteristic excitation by the K alpha line at 1253.6 ev. The electrostatic analyzer was set at 100 ev giving a resolving power of 1.2 ev. The spectra were calibrated by using the Au 4f 7/2 line at 84 ev and this was done by vapor deposition of a small amount of gold on the surface of the sample in the reaction chamber of the instrument. The samples were run at 10^{-6} torr and were maintained at room temperature. The TNT/charcoal samples were ground in a mortar and pestle and mounted with Scotch double-coated

tape 666 on cylinderical aluminum sample holders. The acetone extracts were evaporated directly on the aluminum sample holders. In most cases, spectra were obtained of nitrogen, carbon and oxygen in 10 to 30 minute scans each, depending upon how much sample was available for analysis.

RESULTS AND DISCUSSION

Stability of Surface Area of FS300

Before the study on the regeneration of FS300 involving a water/ acetone system could be conducted, the effect of water, acetone and heat, separately and in combination on the stability of the total surface area was determined. The results are summarized in Table 2.

Since the activated FS300 is relatively hydrophobic, the water molecule does not enter into the microporous structure and is excluded even though its molecular diameter (3.8A) is less than the critical diameter of the micropores, 5-15A. Whereas, acetone, with a molecular diameter of 5.5A, being able to wet the surface of the activated carbon, penetrates into the microporous structure. The removal of acetone from the microporous volume is accordingly achieved only with difficulty, requiring heat. In any case, however, the total surface area is constant by the desorption, with or without heat, of water and of acetone.

Diffusion Studies

Adsorption isotherms were obtained for aqueous TNT solutions onto FS300 of widely different particle sizes to study the effect of diffusion on the rate of TNT uptake. The results are summarized in Figure 1. The maximum value of 0.52 g TNT/g FS300 (44 micron diam) represents approximately a two-thirds coverage of the total surface area, based on close-packed monolayer coverage, and a calculated TNT molecular area of $95A^2$. The remaining one-third area may be considered unavailable to the TNT molecule. According to Calgon, the supplier of FS300, the internal structure of FS300 by volume consists of 21% macropores (>200A diam), 26% (meso) transitional pores (15-200A diam), and 53% micropores (5-15A diam) shown in Table 3. The breakdown of surface areas corresponding to the pore size distribution (column 3) is listed in the last column, showing 87.5% of the area attributed to the micropores, 12% to the mesopores, and 5% to the macropores. Therefore, the third of the surface area not occupied by the TNT molecule could be ascribed to a large portion, viz, 40% of the microporous structure consisting of pore diameters less than the molecular diameter of TNT.

By virtue of the pore diameter distribution of the three designated regions, free movement of TNT is expected in the macroporous region (>200A), incipient steric hindrance in the mesoporous region, increasing progressively in the direction of the microporous region (15-5A) where steric hindrance predominates. The reduction in particle size from coarse to medium presumably removes virtually all of the macroporous structure giving full exposure to the mesoporous section. From the increased adsorption rate and capacity data exhibited by the medium as compared to the coarse, it becomes apparent that some of the meso structure has been opened and made the microporous region more accessible to the TNT adsorbate. The reduction in particle size to fine further increases the rate and capacity of adsorption and hence more of the meso region is eliminated, exposing the microporous region more completely. It should be noted at this point that the process of reducing the particle size is not expected to affect the microporous structure in any way, so that it remains unchanged in all three particle sizes. Apparently, the different rates of TNT uptake by FS300 as a function of particle size (Fig 1) are governed by the diffusion process in the mesoporous region, i.e., the greater the adsorption rate, the greater the diffusion rate, and the greater the accessibility to the microporous region.

As a final note on the diffusion process, it should be emphasized that the observed capacities are independent of the different geometric surface areas of the respective particle sizes. Although the geometric surface areas (calculated), .003, .008 and .08 cm^2/g, respectively, for the coarse, medium and fine particles differ by order of magnitude, the corresponding percent differences with respect to the total surface area of 1000 M^2/g for each of the particle sizes is infinitesimal, viz, 3×10^{-8}, 8×10^{-8} and 8×10^{-7} percentages, respectively.

The effect of particle size of FS300 at different pH's on the rate of adsorption of TNT is graphically depicted in Figures 2 and 3. The adsorption rates for the three different particle sizes in acidic and alkaline media are, in essence, the same (within experimental error) as those reported in neutral medium, pH = 6.3, Figure 1. This forcefully demonstrates the absence of an ionic mechanism in the adsorption and diffusion of TNT from aqueous solution by FS300 and is in agreement with the conclusions drawn from the zeta potential measurements cited below.

The rate of adsorption of TNT as a function of temperature on fine and medium particle size FS300 is shown in Figure 4. The rate of TNT adsorbed for the respective charcoals is independent of temperature, and hence, has no apparent effect on the diffusion process

demonstrated in Figure 1. Normally, the rate of diffusion is increased with increasing temperature. However, concomitantly, the rate of adsorption is decreased with increasing temperature. Fortuitously, for this particular system, these diametrically opposing rates are of equal magnitude and, therefore, cancel each other as depicted.

Deactivation of FS300 Charcoal

Fine, medium and coarse particle size FS300 were subjected to the normal aqueous solution of TNT, allowed to equilibrate, and the adsorbed TNT was then desorbed with acetone. This constituted one cycle (adsorption-desorption). The cycle was repeated on the same batch of charcoal five times, and the surface area was monitored with each adsorption and desorption. The progressive rate of deactivation of FS300 as a function of adsorption/desorption cycles is shown in Figure 5 to be independent of particle size. Deactivation may be looked upon as less being desorbed than adsorbed after each successive cycle. In spite of the fact that the adsorption follows the order, fine> medium> coarse, the desorption is also in the order fine> medium> coarse and, apparently, in identical ratios to their respective adsorption values for all three particle sizes. The adsorption time factor for the different particle sizes is constant and finite, where departure from the time for equilibrium saturation is in the order, coarse> medium> fine which is the reason for the differences in the capacity factor. In particular, at approximately two hours, the fine particle adsorbs TNT to its saturation level, the medium to 60% saturation and coarse to 15% capacity. The importance of minimizing the path length the TNT must traverse to interact with the available microporous surface is demonstrated once again.

But this does not explain why the proportionality of TNT adsorption/desorption remains constant with time for the three different particle sizes. One possible explanation is that the proportionality constant is related to the reaction rate constant of the TNT with the charcoal surface, in that the amount of TNT adsorbed irreversibly is a function of the residence time of that quantity of TNT in the adsorbed state. Accordingly, the amount of TNT desorbed is proportional to the quantity of TNT which is irreversibly adsorbed. Therefore, the rate of deactivation is independent of particle size, but solely dependent on the residence time.

A material balance of adsorbed/desorbed TNT with coarse charcoal is given in Table 4. Column 2 (Sp. adn) shows the specific adsorption of the charcoal decreasing with each successive adsorption/desorption cycle (desorption with acetone). Although the specific adsorption decreases with each successive cycle, the total adsorptive capacity remains constant, i.e., cumulative retained plus adsorbed

TNT (addition of column 2 with column 4 of the prior cycle). However, what is unique is the relationship of the surface area to the repeated cycles. It was previously shown that approximately one-third of the total surface area of FS300, is not available for TNT adsorption. In addition, as a result of the two-third surface area covered by TNT, the entrance to $\sim$ 40% of the microporous structure representing one-third of the total surface area becomes blocked and remains blocked even after desorption, as verified by the argon surface area 699 M^2/g after desorption of TNT/1069 M^2/g virgin FS300, or 0.65.

The surface area decreases after each successive cycle, indicative of progressive plugging, of the micropores by TNT. The specific adsorption, in terms of molecules adsorbed per M^2, is shown in Table 5 (column 4) to decrease proportionately. This is substantiated by the corresponding decrease in the specific adsorption of TNT (column 2) in terms of molecules *adsorbed per residual surface area available* for TNT adsorption (column 3). Based on these results, the deactivation of carbon by TNT appears to be attributable to the progressive irreversible plugging of the overall porous structure by TNT. The last column shows the extent of multilayer adsorption of TNT on the internal surface of the charcoal. Although adsorption from solution is classically thought of as being monolayer, these measurements indicate the erratic multilayer adsorption of TNT, blocking meso as well as microporous structure under equilibrium conditions of saturation.

Since acetone was used to remove TNT from charcoal, it was necessary to see if residual acetone, sorbed in charcoal, would affect the adsorption of TNT. Experiments (Table 4) on medium and coarse FS300 show no significant difference between TNT adsorption on charcoal initially exposed to acetone and then washed with water, and charcoal washed only with water (control). Any changes in adsorption capacity after desorption with acetone, therefore, can be attributed to some interaction of TNT with the charcoal surface.

Electron Spectroscopic Analysis of TNT/Charcoal Interaction

The surface of virgin charcoal was examined to obtain a background reading for the TNT/surface adduct analysis. Figure 6 shows the electron spectra of carbon, oxygen and nitrogen. The presence of oxygen is not too surprising, and it probably is in the form of primarily adsorbed water, plus some carbonyl and hydroxyl functional groups together with organic contaminants. The nitrogen signal indicates the absence of any nitrogen-containing compound.

Explosives generally contain nitrogen in distinct oxidation states which, when subjected to chemical interaction, undergo changes in their oxidation states. The electron spectra corresponding to such induced changes can be recorded by ESCA. TNT contains nitrogen in one oxidation state, N^{+3} of the nitrogen dioxide functional group. The electron spectrum of the TNT used in this study is shown in Figure 7 to contain, therefore, a single peak of 405.6 ev associated with the oxidation state of nitrogen (the small broad peak at approximately 400 ev is a satellite peak not attributable to any oxidation state of nitrogen).

Examination of the TNT in the adsorbed state, after the first adsorption, shows (Fig 8) the major nitro nitrogen peak, N^{+3}; and a broad nitrogen signal of significant proportions, approximately 25%. The assignments of N^{+1} and N^{-1} at 401.0 and 400.0 ev, could be indicative of a nitroso and secondary amine nitrogens, respectively, resulting from chemisorption. An alternative assumption could be made at this point that the apparent reduced form of the nitro nitrogen results from an electron transfer charge complex that is strongly physisorbed. As a further probe into the nature of the TNT surface adduct, an electron spectrum was obtained of the adduct retained by the charcoal after one desorption run with acetone at ambient temperature, and the acetone extract was examined by gas-liquid chromatography (GLC). The TNT removed by acetone elution is, unquestionably, as shown by Figure 9, unaltered TNT which is adsorbed reversibly by van der Waal's forces. The GLC analysis was run over a 30-minute period and no other component was present in the acetone eluent. Since not all of the TNT was desorbed, the retained TNT could be a strongly bound complex of TNT or a chemically bound TNT on the charcoal surface. The electron spectrum of the retained TNT is depicted in Figure 10 and shows the nitro nitrogen peak to be reduced to the same intensity as the broad nitrogen peaks at 401 and 400 ev. Therefore, the retained TNT was indeed some transformation product of TNT. To ascertain whether this was a reaction product that was strongly bound or a chemisorbed species irreversibly adsorbed on the charcoal surface, the charcoal containing the residual TNT adduct was subjected to extraction in a Soxhlet with acetone at 50°C over a 3-day period. The substrate material treated in this manner was examined by ESCA and the electron spectrum (Fig 11) is identical to the one shown in Figure 10. The conclusion drawn from such observations is that this was a chemisorbed reaction product and that the reaction is induced at the charcoal surface.

Infrared and Mass Spectrometric Analysis of TNT/Charcoal Adduct

Proof of the chemisorbed TNT was made using two independent methods of identification, viz, IR and MS techniques. For such

analyses, the sample of charcoal/TNT complex that had been exhaustively extracted with acetone was ground to a fine particle size. For the IR analyses it was pelletized in KBr and for the MS analysis it was introduced directly with the solid probe. The IR spectra of the TNT standard compared with the charcoal/TNT complex is shown in Figure 12. The arrows indicate the points of differences between the two spectra. The bands at approximately 2300 cm^{-1} could be due to a coupling of the TNT molecule. This is supported by the MS data cited below. The band at 1700 cm^{-1} shows some oxidation of TNT and reduction of the NO_2 group to NO at 1300 cm^{-1}. The differences in the adsorption band structure at the lower frequencies are indicative of induced electronic charge density perturbations with delocalized π orbitals of the TNT molecule in the adsorbed state.

The overall MS fragmentation pattern of the TNT complex adduct (Table 7) is more extensive than that of the TNT standard. The mass of 256 which is larger than the molecular weight of TNT (228) is attributed to the fragmentation of at least a dimer of TNT involving a coupling of -N = N- type shown above in the IR spectrum. Therefore, these alternative independent methods of analyses support the conclusion drawn from the ESCA data that the TNT complex at the substrate charcoal surface is indeed a chemisorbed species. That this chemisorbed species is of a complex nature is demonstrated by the multiplicity of induced chemical changes of the TNT molecule involving oxidation, reduction and coupling reactions products; and as such the species are irreversibly adsorbed.

Characterization of FS300 Charcoal Surface

Water adsorption isotherms were used to characterize the surface properties of virgin FS300 charcoal and acetone eluted TNT-FS300 samples. The approach for this analysis was two-fold: low pressure water adsorption isotherms, expressed in units of molecules adsorbed per unit area, which were expected to reveal the surface polar site concentration; and the high pressure water adsorption isotherms were expected to show the degree of porosity of the FS300. The concepts which, a priori, justify this approach are as follows: the adsorption of TNT on charcoal always results in an appreciable decrease in surface area. Since the FS300 charcoal is reported to be of a highly porous structure, and since the adsorption of molecules such as TNT on an "open" surface is not expected to result in a decrease in surface area, it must be concluded that the mechanism of TNT adsorption involves the closing of pores. The progressive cycling of the acetone-eluted TNT/FS300 samples, furthermore, results in increasing concentrations of irreversibly adsorbed TNT and a decreasing efficiency for further adsorption of TNT. The irreversibly adsorbed TNT must be due to chemisorption onto active polar sites. Hence, a knowledge of

the polar site concentration and the pore size distribution as a function of the concentration of irreversibly adsorbed TNT becomes important for deriving a mechanism for the decreased efficiency of the charcoal for adsorbing TNT.

Gas adsorption isotherms were used to analyze the pore size distribution of a solid surface, using the Kelvin equation which predicts the condensation pressure of a vapor as a function of the radius of the pore and the contact angle of the condensed liquid on the pore surface:

$$\ln p/p_o = \frac{-2V\gamma}{RT\ r\cos\theta}$$

where:
- p = equilibrium vapor pressure of adsorbate
- p_o = saturation vapor pressure of adsorbate
- γ = surface tension
- V = molar volume
- R = constant
- T = temperature
- r = radius of capillary
- θ = contact angle of condensate with surface.

Figure 13 presents the results from application of the Kelvin equation for water vapor where the condensation pressure is plotted as a function of pore radius for contact angles of 0° and 45°. The lower limit of pore radius analysis is 11A because the condensed adsorbate does not behave as a liquid in smaller pores. The upper limit of analysis is about 100A because the condensation pressures become relatively insensitive to pore radius above this value.

Figure 14 presents the water adsorption isotherms measured on virgin FS300, TNT saturated FS300 (first adsorption), and on 2 and 5 cycle acetone-eluted TNT/FS300. Both the virgin and acetone-eluted TNT/FS300 samples show sharp rises in the adsorption isotherms occurring below 16 mm, and a pronounced hysteresis loop in the desorption branches of the isotherms. Both of these factors indicate a high degree of porosity of the charcoal samples in the pore radius range of 11 to 100A with most of the pores being below 40A as determined from the Kelvin equation. The pronounced hysteresis, at lower pressures, indicates that the pore openings are smaller than the body of the pores since the adsorption is controlled by the pore body dimensions while the desorption is controlled by the pore opening. The cycled TNT/FS300 samples also show a shift in the adsorption and desorption branches of the hysteresis loop to higher vapor pressures, as well as a decreased capacity for water adsorption, with both

factors being enhanced with successive cycles. These factors, together with the decrease in surface area of the cycled TNT/FS300, lead to the conclusion that the plugging of the smaller pores, i.e., less than 40A, is undoubtedly due to the irreversibly adsorbed TNT. The adsorption-desorption isotherm of water on the TNT saturated FS300 showed a large decrease in its capacity to adsorb water and very little hysteresis. This decrease in water adsorption capacity, along with the measured decrease in specific surface area for this sample, is due to an extensive plugging of pores by adsorbed TNT. The fact that no sharp rise was observed in the isotherm and that very little hysteresis was detected in the pore size range of 11A to 100A, as determined by the Kelvin equation, indicates that physically adsorbed TNT has a tendency to plug up larger pores, at least up to 100A.

The water adsorption results presented in Figure 14 are shown in Figure 15 in the low vapor pressure region below 2 mm, and the water adsorbed is expressed in units of amount adsorbed per unit area, i.e., molecules adsorbed per $100A^2$. The results in Figure 15, which are intended to define the intensive hydrophilic characteristics of the charcoal surface, are interesting from two points of view. The results on the TNT saturated charcoal show that the reversibly adsorbed TNT, which predominates over the chemisorbed or irreversibly adsorbed TNT, is strongly hydrophilic compared with the virgin charcoal surface. The second and fifth cycle samples, which contain different concentrations of irreversibly adsorbed TNT, however, show very little change in surface hydrophilicity as compared with the virgin charcoal. These results suggest that the irreversibly adsorbed TNT, which is itself polar and which is responsible for drastic decreases in specific surface area due to the blocking of pores, either chemically interacts with the low concentration of surface polar sites or prevents the adsorption of water on polar sites present in the small pores. In either event, the introduction of a polar site due to adsorbed TNT appears to result in a loss of polar site present on the charcoal surface.

A further analysis concerning the change in porosity of the charcoal as a function of adsorbed TNT can be made from the water adsorption results. A necessary assumption which must be made is that the hydrophilic character of the charcoal surface does not change as a function of adsorbed TNT. Figure 15 shows this assumption is reasonably good for all samples except the TNT saturated charcoal which exhibits a higher degree of surface hydrophilicity. The analysis is made by comparing the shape of each isotherm with the virgin charcoal in the water vapor pressure range of 8 mm to 19 mm (Fig 14). Any decrease in the amount adsorbed in 1 mm increments is attributed to a decrease in pore volume within that incremental

pressure range which may be assigned an effective pore diameter according to the Kelvin equation described above and the results of this theory shown in Figure 13. The results of this analysis, presented in Figure 16, shows that the second cycle sample undergoes a decrease in porosity in the range of 11A or less up to 22A. The fifth cycle sample undergoes a larger pore reduction in the range of 11 to 33A. The TNT saturated charcoal shows the largest decrease in pore volume and in the higher pore diameter range of 11A to over 50A. All of these results are consistent with what has been observed in the water adsorption isotherms and the specific area measurements.

The electrophoretic properties of charcoal as a function of pretreatment conditions and in different liquid media were investigated in order to determine if the solution adsorption properties of TNT on charcoal are controlled by coulombic forces. The surface potential as the solid/liquid interface for the purposes of this investigation may be equated to the zeta potential, ζ, which is defined by the following equation:

$$\zeta = \frac{4\Pi \eta v}{D E}$$

where η is the viscosity of the liquid, v is the electrophoretic velocity of the particle, D is the dielectric constant of the liquid, and E is the applied potential gradient. The dispersed charcoal particles were measured in distilled water and in a 130 ppm solution of TNT. The results presented in Table 8 are represented in electrophoretic mobility units, U_e, where $U_e = v/E$, and in zeta potential. The results show that all the particles are negative and undergo very little change in the magnitude of the surface charge under the various conditions of adsorbed and desorbed TNT. Apparently the acetone treatment has no effect on the surface charge even after five cycles of treatment, and the decreased adsorption capacity of the charcoal for TNT is not related to any changes in the surface charge.

Mechanism of TNT Adsorption on FS300

A brief review of the more fundamental physical and chemical properties of activated carbon surfaces is presented as a background in support of the interpretation of the results obtained in this study. Activated charcoal, as manufactured by the carbonization and oxidation by gases of bituminous coal results in a highly porous structure of large internal surface area. The porosity is created by the carbonization and oxidation of intermicrocrystallites. The

extensive interparticle surface is very heterogeneous in nature, consisting of irregular basal planes and a multiplicity of edges at the microcrystallites (Ref 2). Each microcrystallite is composed of irregular packets of graphite-like layers with a diameter and height usually less than 100A. A graphitic layer, which may be regarded as a very large polynuclear aromatic molecule is depicted in Figure 17. The tetrahedral bonding of carbon in the irregular microcrystallite is considered to be highly distorted and strained, departing, thereby, from the ideal graphitic structure. The carbon atoms at the edges of the graphitic planes, having reduced coordination numbers (unshared electrons), act as free radical or high energy sites. As a result, the activated charcoal contains impurities at the surface in the form of functional groups, some of which are derived from substances added to catalyze the carbonization and oxidation steps. Some of these functional groups have been characterized by Donnet (Ref 3) as comprising four different types:

R-OH Hydroxyl function

R-COOH Carboxyl function

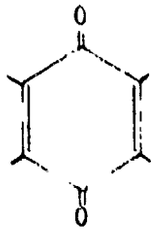

Quinonic function

Lactonic function

The surface structure according to Boehm (Ref 4) may be of the open or lactonic form, as shown in Figure 18. The postulated structures are for carbon black, but may well be applicable to a charcoal surface. However, the model is limited to acidic functions and does not include any of the basic oxides known to be present on activated surfaces (Ref 5). Carefully outgased carbon, after activation at 800°C to 1000°C could exhibit basic properties, depending on the temperature of reaction with oxygen. The basic oxide thus formed could behave as a Lewis base, donating an electron to the acceptor molecule and forming a covalent bond.

Carbon surfaces have been shown to contain some surface free radicals. Their numbers may be as great at 1-2 x 10^{20}/gram of carbon, which can be measured by ESR (Ref 6). The unpaired electrons of carbon are capable of forming a covalent bond with organic radicals (induced). The free radicals appear to be related to the amount of quinone function present. The proposed forms (Ref 7) are radical-quinone or an aroxylic type configuration:

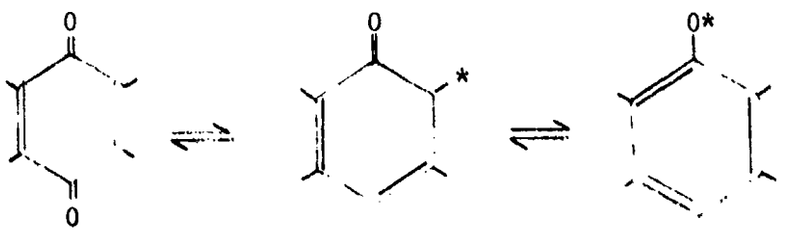

The effect on the adsorption process of the pore structure and surface area should be considered in conjunction with the chemical nature of the surfaces of activated carbons. It is apparent from the pore size distribution data shown in Table 3 that the major contribution to surface area is located in pores of molecular dimensions (micropores, 5-20A diam). Hence, a molecule, because of steric effects, cannot penetrate into a pore smaller than a certain critical diameter. Therefore, for any molecule the available surface area for adsorption can exist only in pores which the molecule can enter. An attempt to illustrate this concept is shown in Figure 19 for the case in which two adsorbate molecules in a solvent (not shown) compete with each other for adsorbent surface (Ref 8). Because of the irregular shape of both pores and adsorbate molecules, the fine pores can be blocked by the larger molecule, either blocking and/or preventing entry of the smaller adsorbate.

In summary, the chemical reactivity of activated carbons is well established experimentally, in spite of the fact that the

mechanisms involved are not completely understood. This reactivity is due in part to the presence on the surface of chemical functions, both acidic and basic, free radical acceptors, and high energy sites at edges, cracks, crevices, crystal lattice defects, irregularities and distortions of the microcrystallites. Also, the microporous structure, containing constrictions narrow enough to hinder the free passage of adsorbates, renders some of the surface unavailable for adsorption. Certainly, the potential fields from the opposite walls of the micropores tend to overlap, so that the attractive forces acting on the adsorbate molecules will be increased as compared with those on a relatively open surface. Adsorbate interaction with the surface will, accordingly, be diverted to the realm of strongly bound physi- and chemisorption. In light of these concepts on the physical and chemical properties of activated carbon surfaces, the data obtained in this study on the interaction of TNT with the FS300 surface can now be evaluated and a meaningful mechanism postulated.

Initially, as the TNT molecule diffuses into the internal surface of FS300, it traverses freely into the macroporous structure (>200A diam) which comprises large avenues leading to the mesoporous region (200-15A diam). Then, movement of the TNT molecule is partially restricted as it penetrates further into the narrower portions of this region. Finally, continued diffusion into the largest surface area section, consisting of micropores (15-5A), proceeds with increased steric hindrance until the TNT molecules (9.8 x 9.8A) arrives at pore openings with diameters in the vicinity of 10A, beyond which it cannot penetrate. As a result, TNT adsorbs at these constricted pore openings where the potential force field for adsorption is strongest, approaching 4 Π geometry, and chemical reactivity is promoted as a function of residence time. This takes place at pore diameter openings of 10-12A which blocks off approximately 40% of the microporous surface area or virtually 30% of the total surface area (including the meso and macroporous sections). Progressive filling of pores by chemi- and strong physisorption follows with continued exposure to the diffusing TNT. But, as the remaining available pore diameter structure becomes relegated to the larger dimensions, (>10-12A) the interaction of TNT with the surface is via energy sites consisting of distortions, cracks, crevices, corners, edges and crystal lattice defects of the microcrystallites. In addition, functional groups at these energy sites (resulting from the process of activation by combustion and oxidation) in the form of basic as well as acidic oxides, and perhaps free radical acceptors, react with the NO_2 functional group of TNT. The ensuing reactions entail the formation of reduced products of TNT of the nitroso and amine types; oxidation of the methyl group to TNBA (Ref 8); and coupling reactions resulting in at least a dimer, all of which are irreversibly bound to the surface and further reduce the adsorptive

capacity of FS300 after regeneration by solvent extraction. The process of adsorption continues at sites with decreasing potential field strength to the point where, at their maximum values, only strong physisorption takes place.

As a further insight on the interaction of TNT with the surface of FS300 resulting in the irreversible degeneration of its adsorptive capacity, the reactivity of TNT with the basal planes of the microcrystallites was investigated. This was accomplished by running adsorption/desorption cycles on graphite. Graphite has a uniform surface consisting of regular planes of the polynuclear aromatic configuration. Figure 20 is a complete krypton adsorption isotherm of the graphite employed. The shape of the isotherm is indeed that of a uniform surface with a minimal content of functional groups apparently confined only to the edges of the planes. Hence, any measurable chemical reactivity would be limited primarily to the basal planes containing π bonding orbitals. The graphite was cycled twice and the specific adsorption remained constant and was found to be comparable to that of FS300 on a unit area basis. However, the desorption of TNT was quantitative after each adsorption, signifying no TNT retained by the graphitic surface. The electron spectrum of the nitrogen signal on the surface after the second desorption was of background proportions. The inference drawn from these results is that the TNT does not react with the π bonding orbitals of the uniform portions of the basal planes in ES300.

The reversibly (physi-) adsorbed TNT is removed efficiently by acetone extraction, whereas the chemisorbed species are not extracted. Therefore, any physisorbed TNT blocked by chemisorbed TNT at pore constrictions is prevented from being eluted by the acetone. Hence, the degeneration of the adsorptive capacity of FS300 becomes irreversibly cumulative.

The water adsorption studies support the adsorption/desorption cycling data indicating the progressive rendering of the surface nonporous; and that the TNT increasingly adsorbs irreversibly in the pore diameter range below 30Å, effectively reducing the capacity of the FS300 for further TNT adsorption.

CONCLUSIONS

Diffusion plays an important role in the adsorption process of TNT on FS300. The reduction in particle size shortens the path length of the mesopore structure, allowing TNT to diffuse more directly into the microporous region where the major part of adsorption takes place. Accordingly, saturation is attained over shorter time periods, reducing the residence time of TNT in the adsorbed

state. As a result, there is an associated reduction in chemical reactivity favoring higher levels of reversibly adsorbed TNT; and increased adsorptive capacities by as much as 50% are attained between regeneration cycles of the TNT-saturated FS300 by acetone solvent extractions. Therefore, a marked improvement in the performance of FS300 for the removal of TNT from wastewater effluents could be achieved by the reduction of particle size to a workable diameter of 420 microns, and using acetone as a solvent to regenerate FS300 for at least five cycles before disposition.

TNT adsorbate molecules will be attracted first to regions of the surface which have the highest energy. Therefore, at the low concentrations encountered in the wastewaters, high energy surface area in the micropores may be the dominant factor determining equilibrium capacity, rather than total surface area in all pores. Consequently, there should exist an optimum distribution for the TNT adsorbate which will give maximum adsorption with minimum retentive forces. However, this approach would minimize but not eliminate the chemical interaction of TNT as a strongly electrophilic oxidant with an activated carbon surface. Additionally, what must be accomplished is the pacification of the various functional groups and high energy sites associated with the carbon atoms at the surface having incomplete coordination numbers. More specifically, a number of surface treatments will be performed and the surface properties of the pretreated charcoal will be investigated with respect to porosity, surface area and the polar character of the surface. This approach is expected to lead to an identification of the surface sites which are responsible for the irreversible adsorption of TNT and will result in a method for the desensitization of these sites. In this manner, TNT interaction would be completely confined to reversible adsorption making possible the feasible regeneration of carbon by on-column solvent extraction with acetone. These objectives are currently being pursued in Part II of this study on carbon regeneration.

REFERENCES

1. W.S. Layne and J. Tash, Mason-Hanger, Silas Mason Company, Inc., Middletown, IA, February 1976

2. V.L. Snoeyink, W. J. Weber and H.B. Mark, Environ. Sci and Tech, 3, 918 (1976)

3. J.B. Donnet, "Carbon" Vol. 6, pp. 161-176, Pergamon Press (1963), GB

4. H.P. Boehm, Angew, Chem. 78, 617 (1966)

5. R.W. Coughlin and F.S. Ezra, Environ, Sci and Tech, 2, 291 (1968)

6. M. Szware, J. Polym Sci, 19, 589 (1954)

7. J.B. Donnet, G. Heinrich and G. Riess, Rev Gen Caout, 38, 1803 (1962)

8. Calgon Bulletin, "Basic Concepts of Adsorption on Activated Carbon"

9. Private communication with Dr. L. Kaplan, Naval Surface Weapons Center, White Oak, Silver Spring, MD, Nov 1975

Table 1

UV analysis of aqueous TNT solutions

TNT, ppm Taken	Found	% recovery
8.1	7.9	97.5
5.0	5.0	100.0
10.1	9.7	96.0
4.0	4.1	102.5
2.0	2.1	105.0
10.1	10.5	104.5
10.1	10.2	101.0

Average recovery 100.7
S = 3.2

Table 2

Stability of FS300 surface area

FS300 pre-treatment	Surface area M^2/g + 25 M^2/g
Virgin FS300	876
Virgin FS300 heated 105°C/16 hrs	924
Heated 105°C/16 hrs, water-washed + 105°C/16 hrs	855
Heated 105°C/16 hrs, water-washed, air-dried	875
Water-washed, air-dried	820
Water-washed, 105°C/16 hrs	875
Acetone-washed, air-dried	650
Acetone-washed, air-dried, 105°C/16 hrs	850

Table 3

Pore size distribution of FS300

Pore category	Pore volume c/g	Pore diameter (angstrom)	Surface area m^2
Macro	0.215	>200	5
Meso (transitional)	0.172	15-200	120
Micro	0.438	5-15	875

Table 4

Process of deactivation of coarse FS300 by TNT adsorption

No. cycle	Sp. adn. g/g	ΣD M^2/g	Cumulative retained sp. adn.	Total sp. adn. sp. adn. & cum. ret. sp.adn.
1	.36	890	.12	.12
2	.29	818	.14	.41
3	.25	701	.18	.39
4	.15	570	.19	.33
5	.14	541	.25	.33

$\Sigma_{vc} = 1098\ M^2/g$

Table 5

Effect of adsorption-desorption cycling on medium FS300

No.cycle	Sp.adn. g TNT/g FS300	Σ^b (M^2/g) Acetone-eluted TNT/FS300	Molec.TNT/M^2 x 10^{18}	Σ^b (M^2/g) TNT/FS300
0	-	1069[a]	-	-
1	0.48	699	1.78	57
2	0.45	597	1.70	41
3	0.37	556	1.64	63
4	0.24	529	1.14	122
5	0.22	470	1.10	140

[a]Total surface area of Virgin FS300.

[b]Surface areas determined by low temperature argon adsorption.

Table 6

The effect of pre-adsorbed acetone on the adsorption of TNT on FS300

		Specific adsorption, g TNT/g FS300	
	Adsorption, hrs	Pre-exposed to acetone	Control
Medium FS300	6	0.32	0.36
	24	0.41	0.41
Coarse FS300	48	0.36	0.33

Table 7

Mass spectra of charcoal/TNT complex

Major peaks (M/E)

TNT	Complex
227 (M^+)	256
210	242
193	228
180	209
134	99
89	98
63	59
51	58
39	43

Table 8

Electrophoretic properties of charcoal FS300

Solvent	Pre-treatment	Electrophoretic mobility, mm cm/volt sec	Zeta pot, mV
Distilled water	None	-2.4	-34
Distilled water	TNT (.37)	-2.6	-37
Distilled water	Acetone	-2.5	-35
Distilled water	TNT + acetone	-2.8	-40
Distilled water	5th cycle	-2.3	-33
Distilled water	6th cycle + TNT	-2.0	-29
130 ppm TNT/H_2O	None	-3.1	-44
130 ppm TNT/H_2O	TNT (.37)	-2.4	-34
130 ppm TNT/H_2O	Acetone	-2.6	-37
130 ppm TNT/H_2O	Acetone + TNT	-3.1	-44

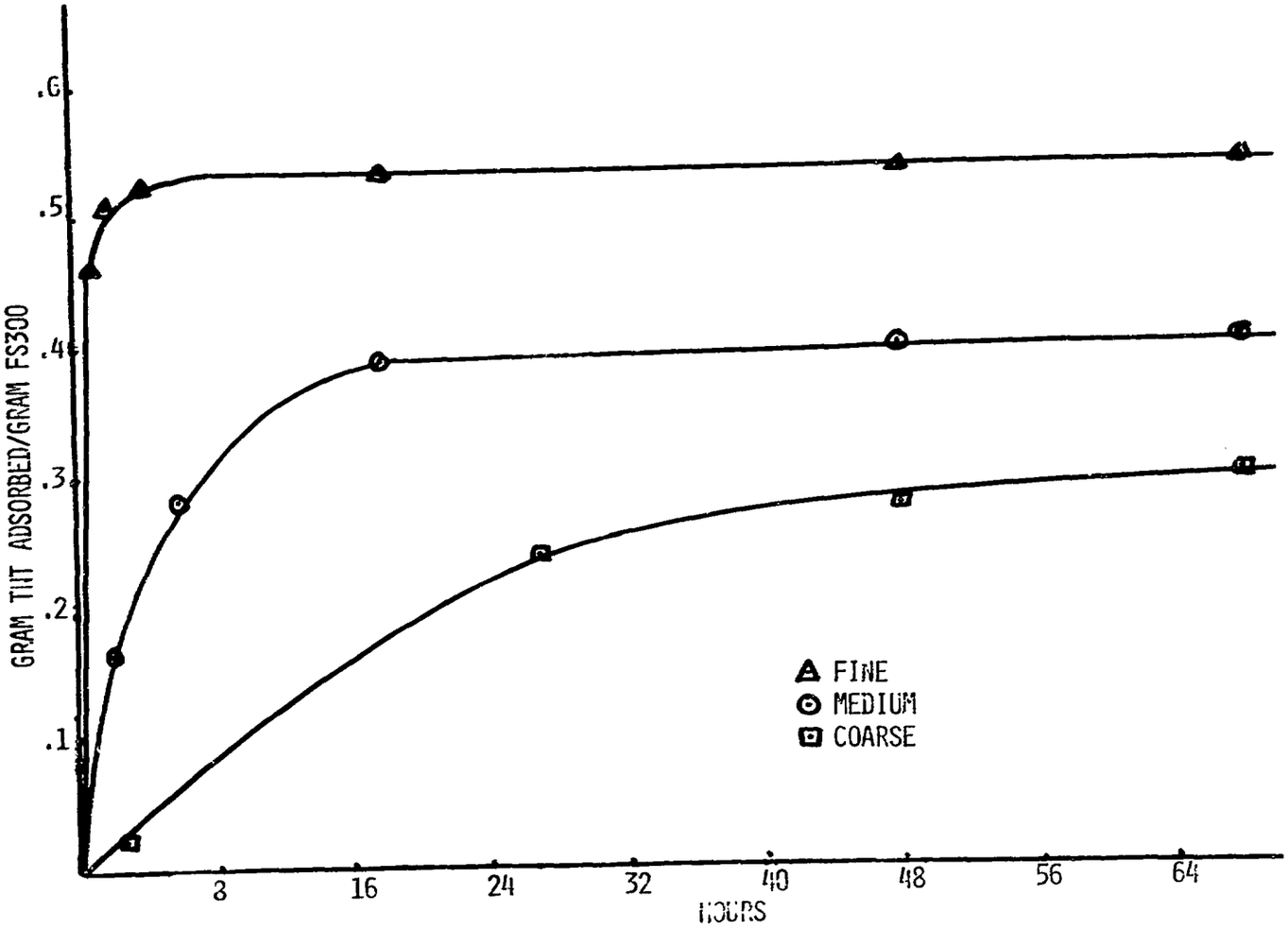

Fig 1 Effect on adsorption rate of TNT by particle size of FS300 at pH = 6.3

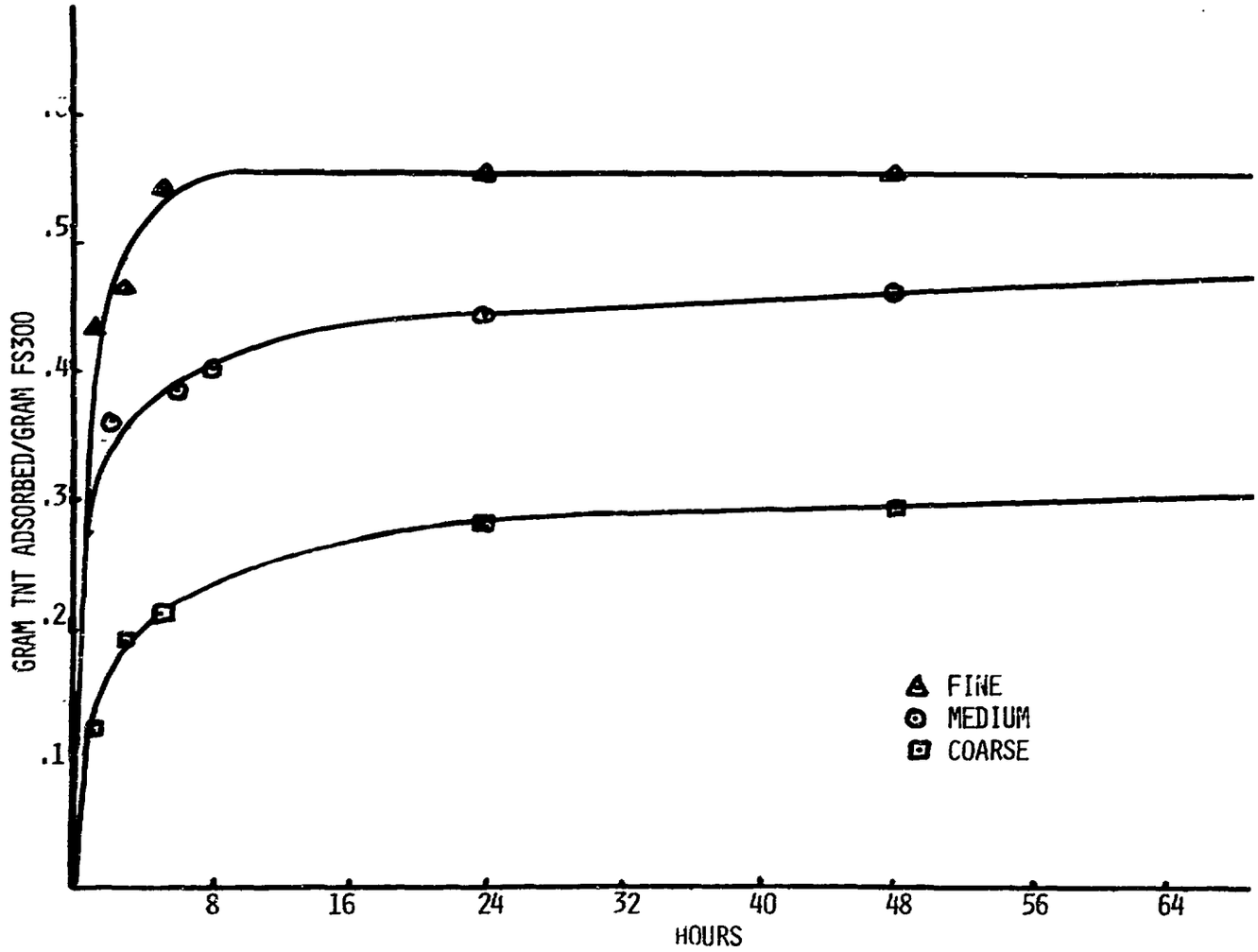

Fig 2 Effect on adsorption rate of TNT by particle size of FS300 at pH = 10.5

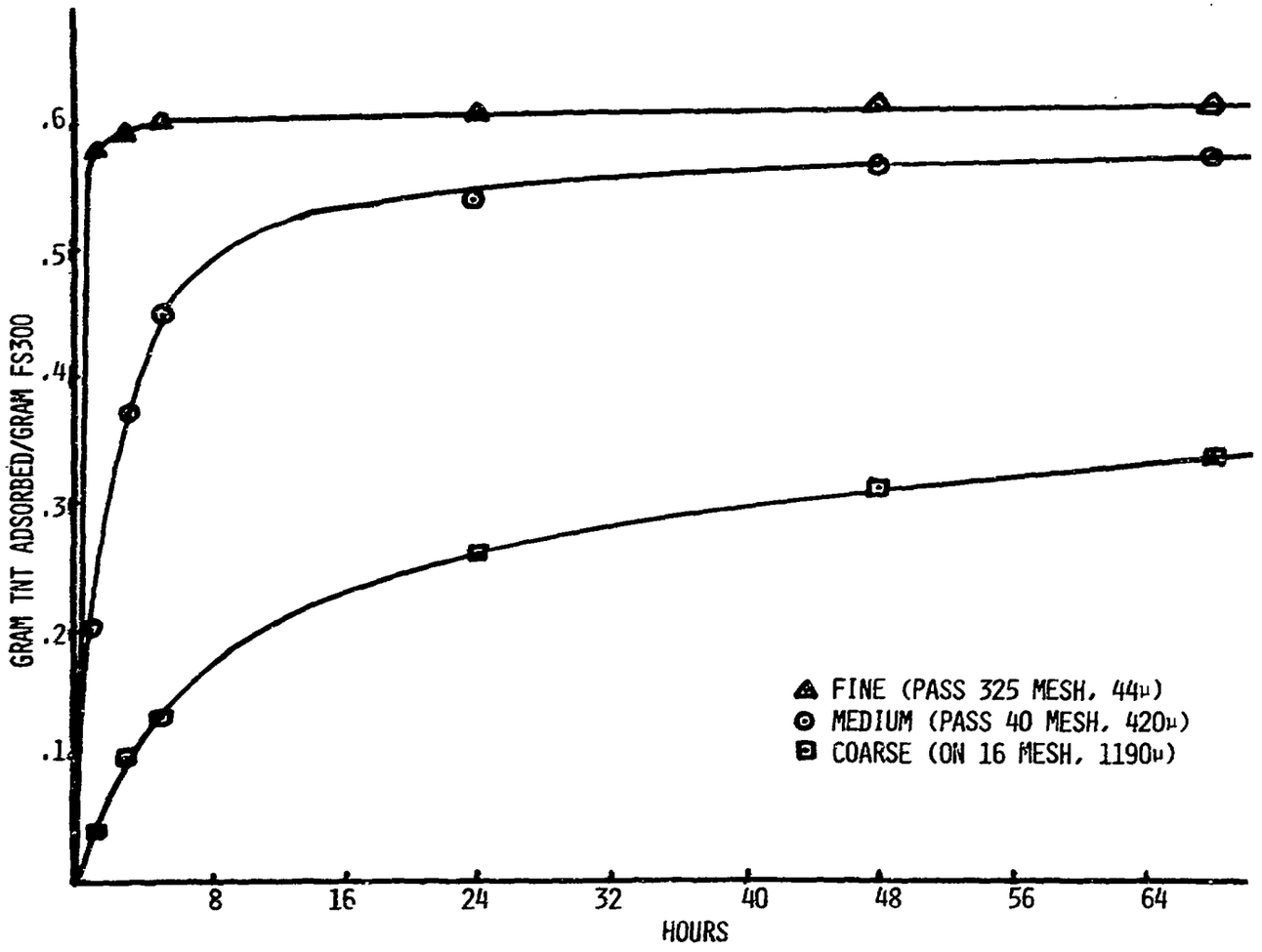

Fig 3 Effect on adsorption rate of TNT by particle size of FS300 at pH = 2.8

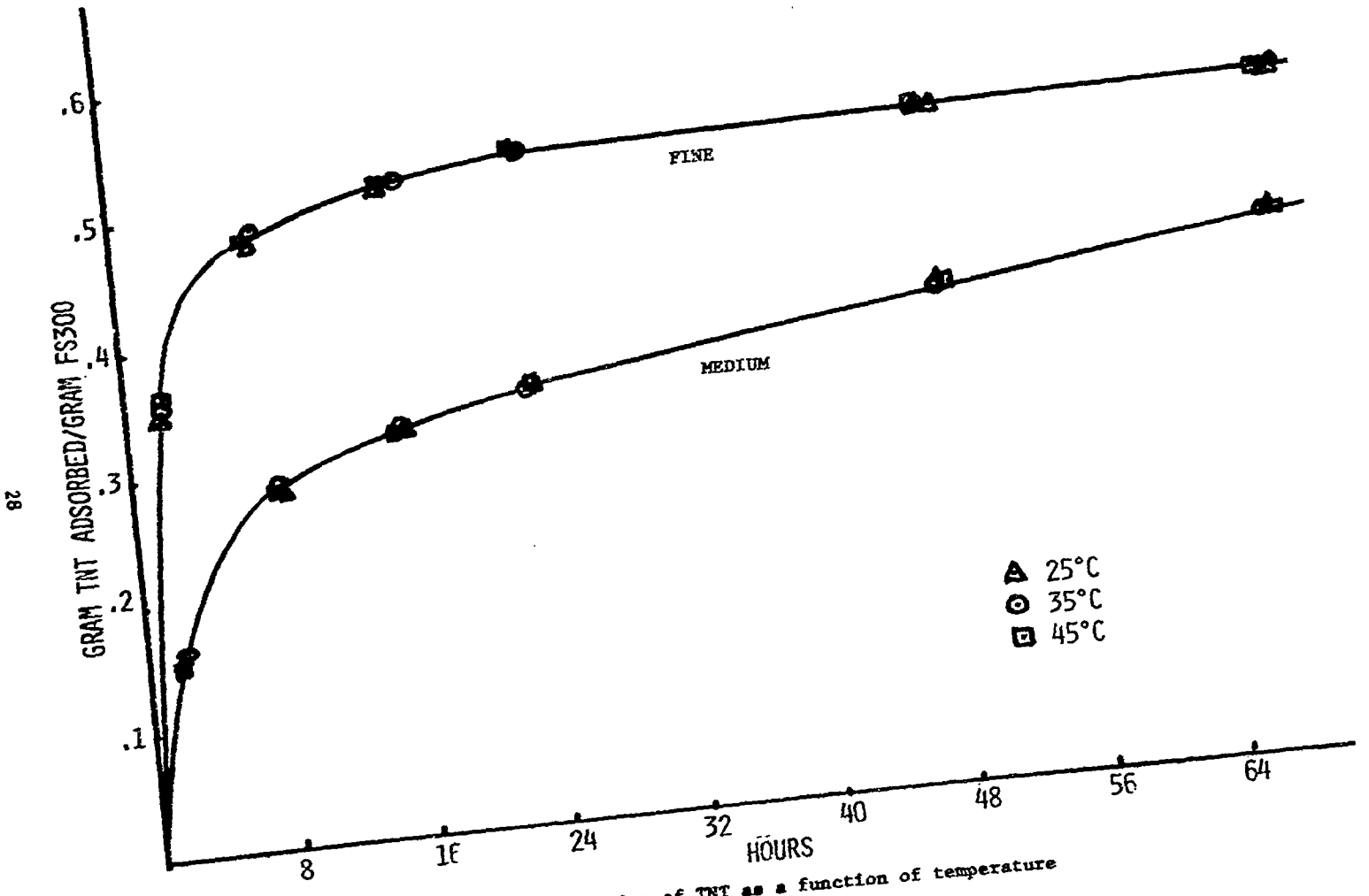

Fig 4 Rate of adsorption of TNT as a function of temperature

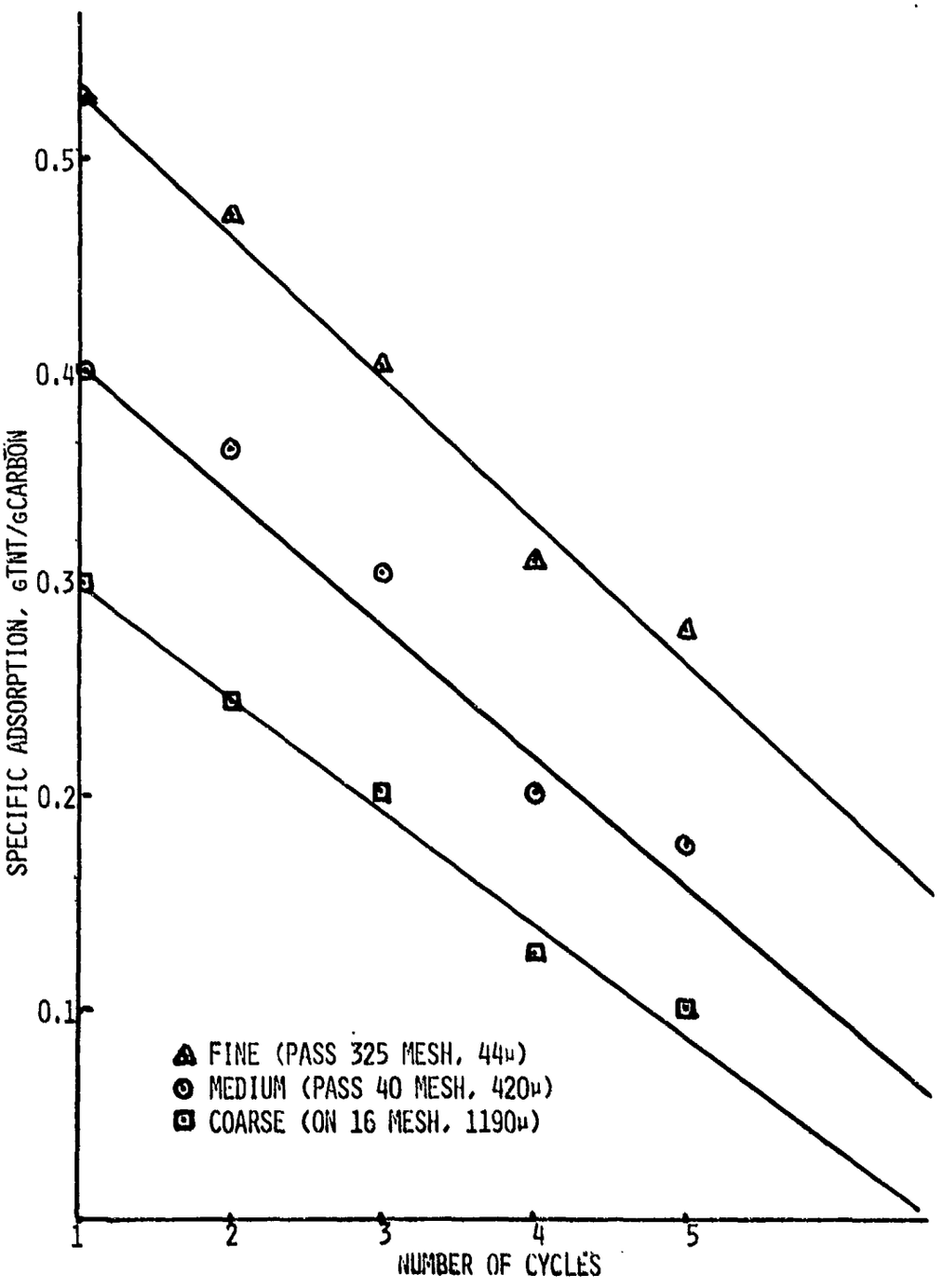

Fig 5 Deactivation as a function of adsorption/desorption cycle and particle size

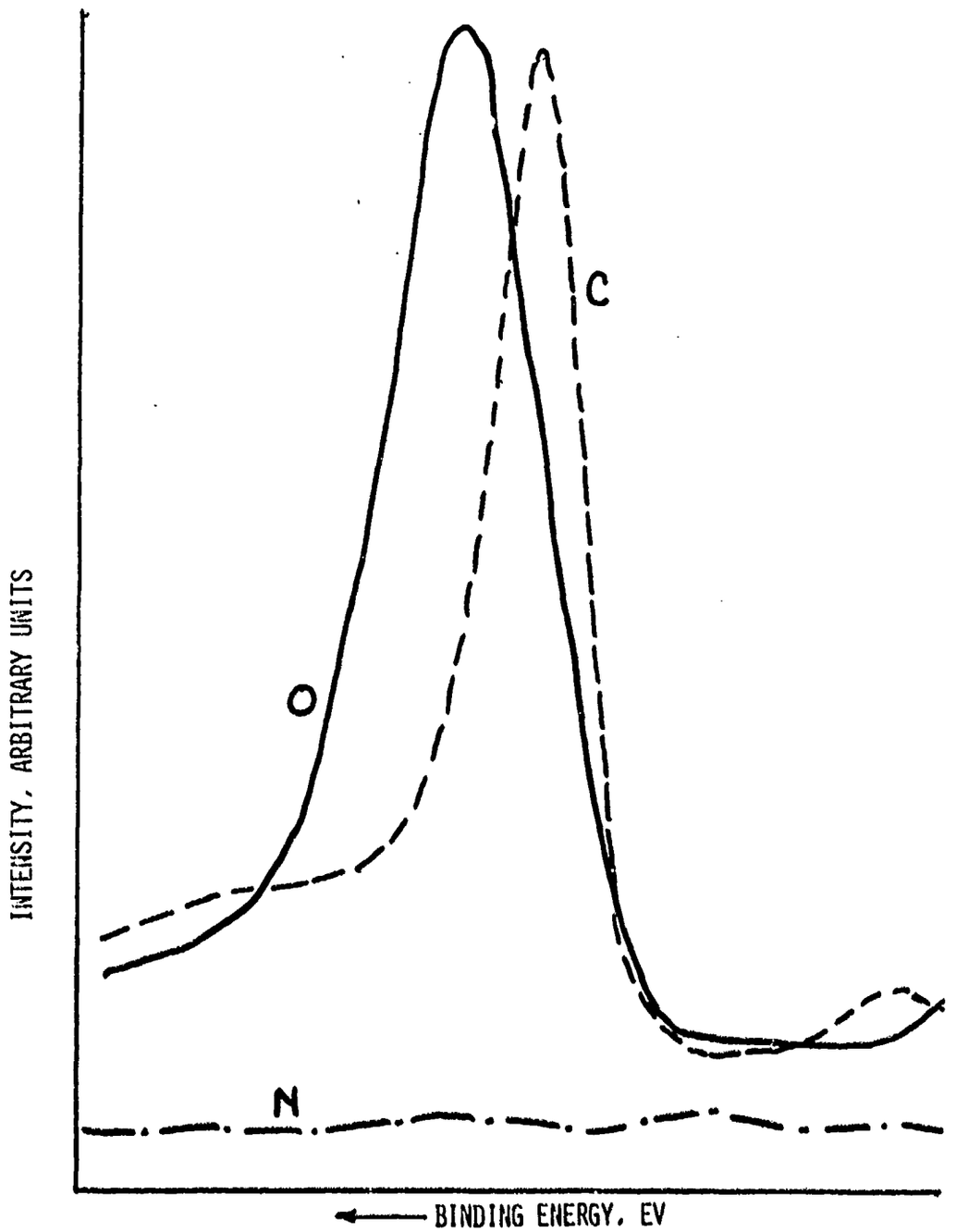

Fig 6 Electron spectra of virgin FS300 as received

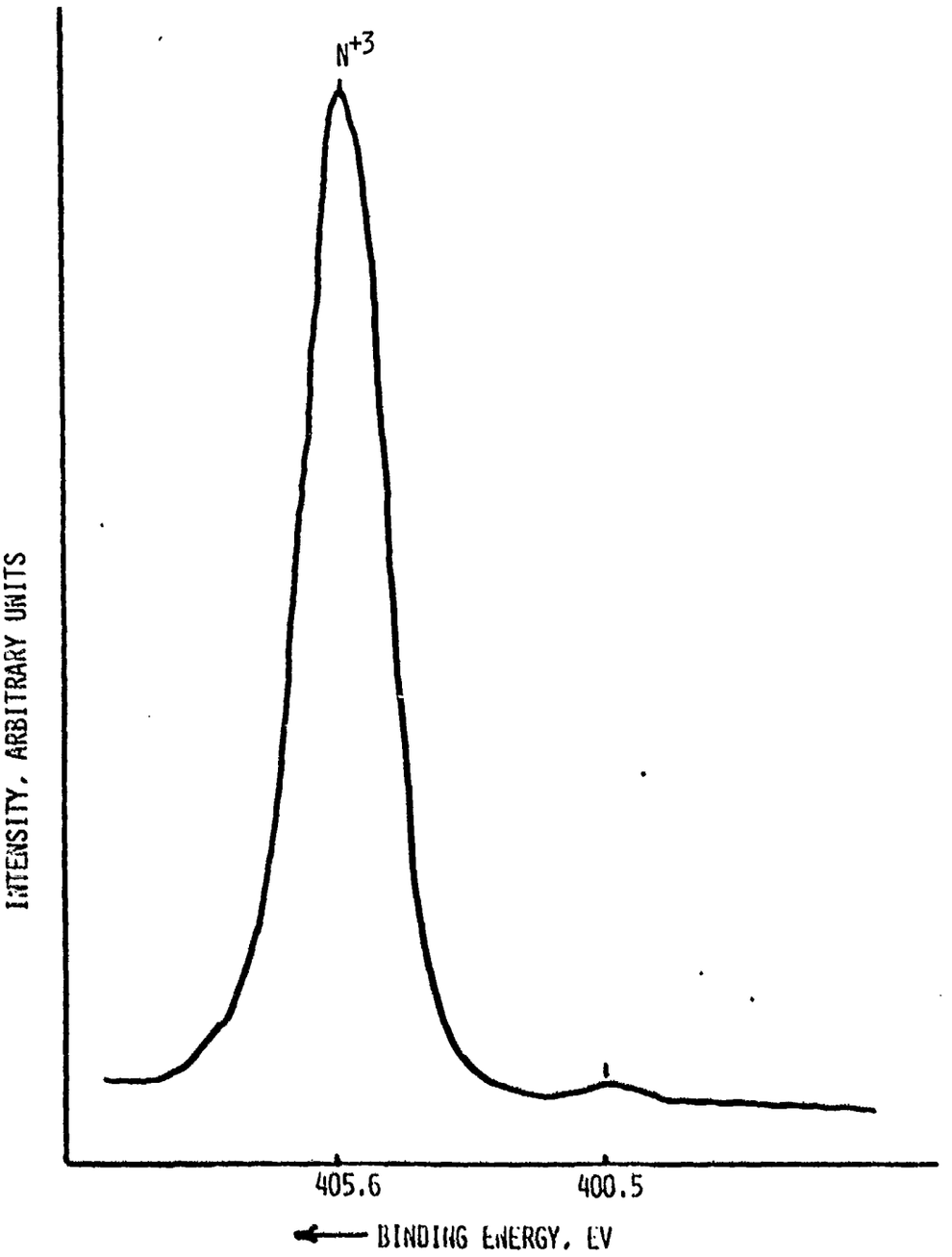

Fig 7 Electron spectrum of TNT standard

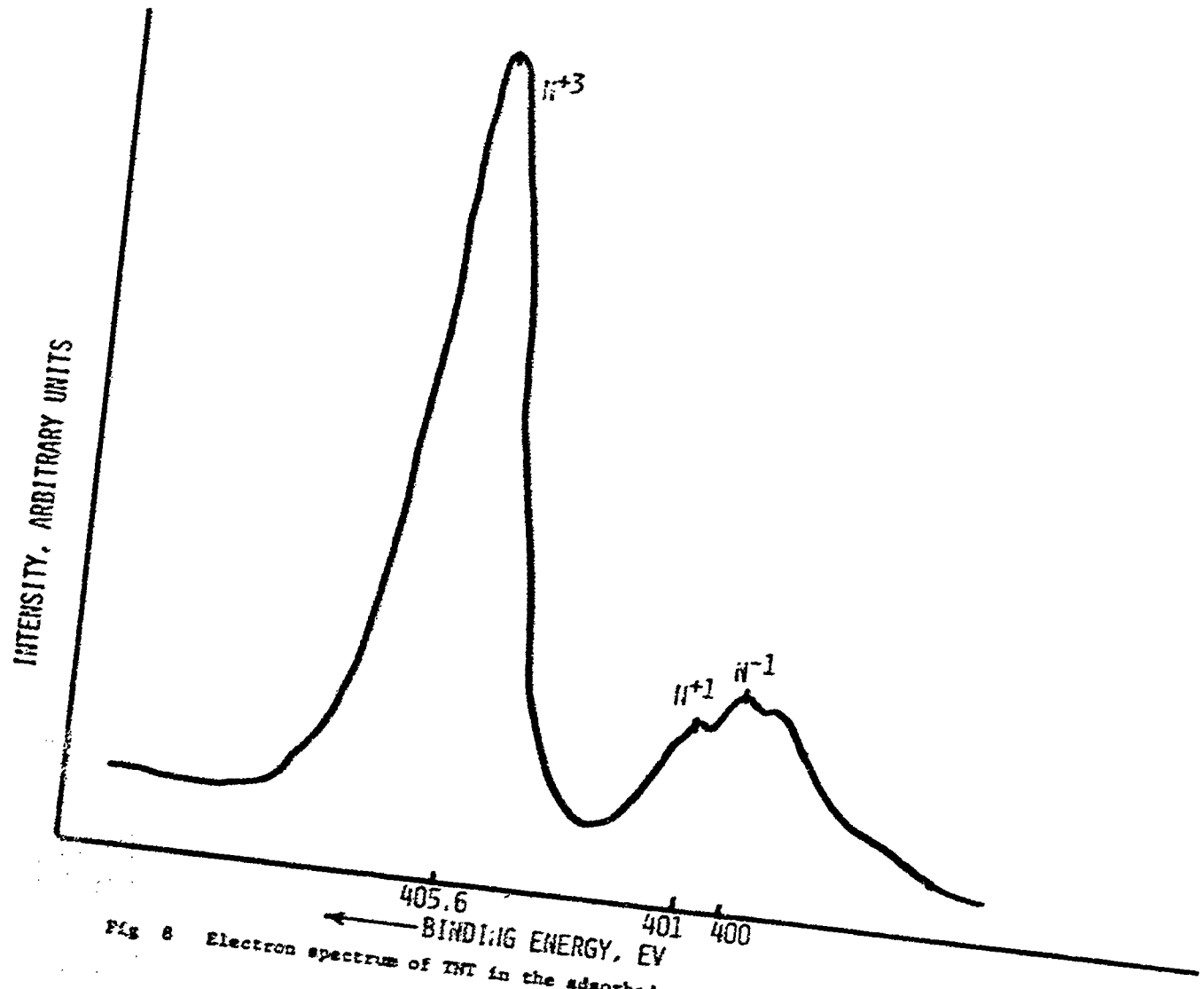

Fig 8 Electron spectrum of TNT in the adsorbed state on FS300 surface

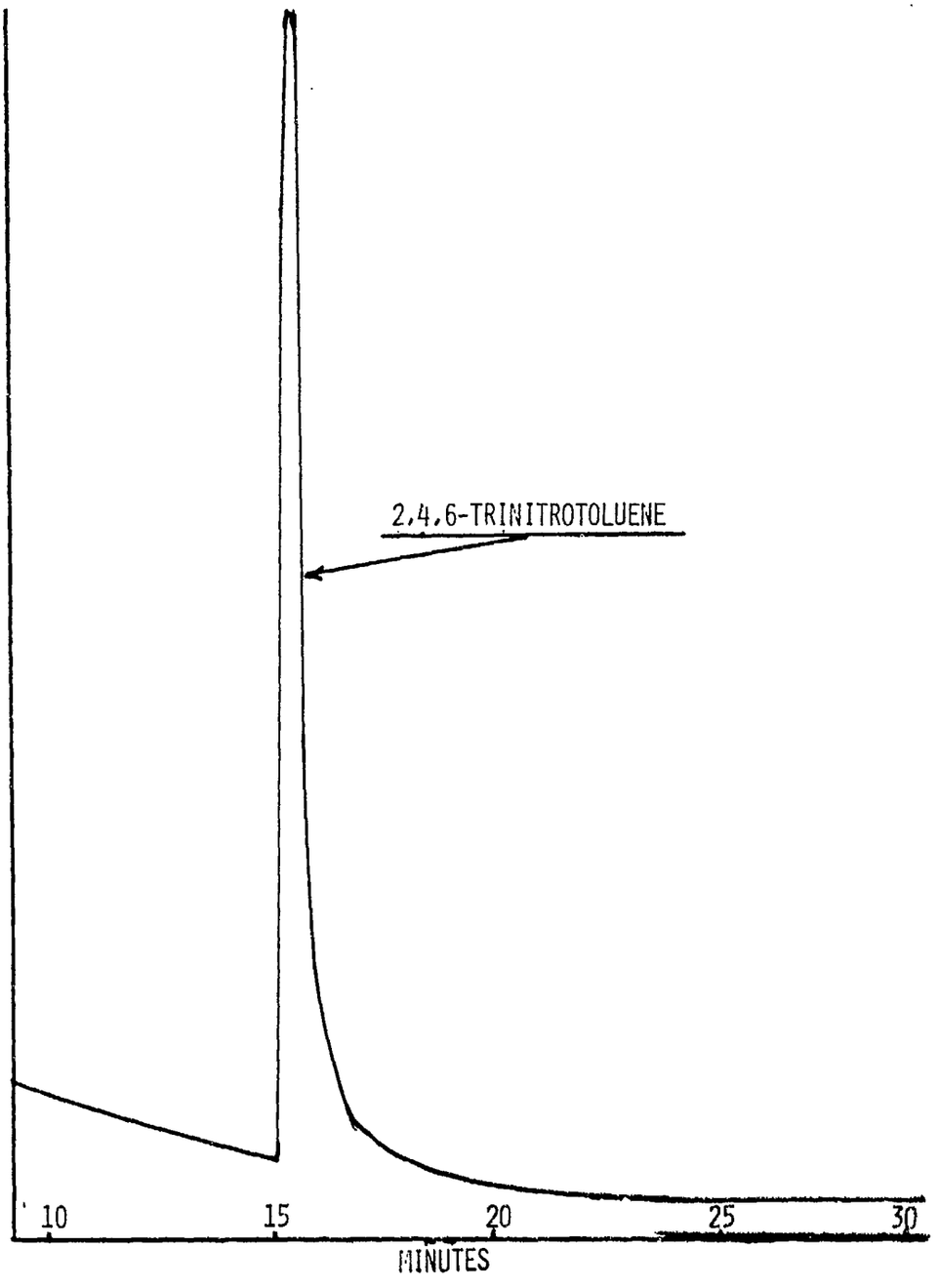

Fig 9 GLC analysis of acetone eluent of TNT-saturated FS300

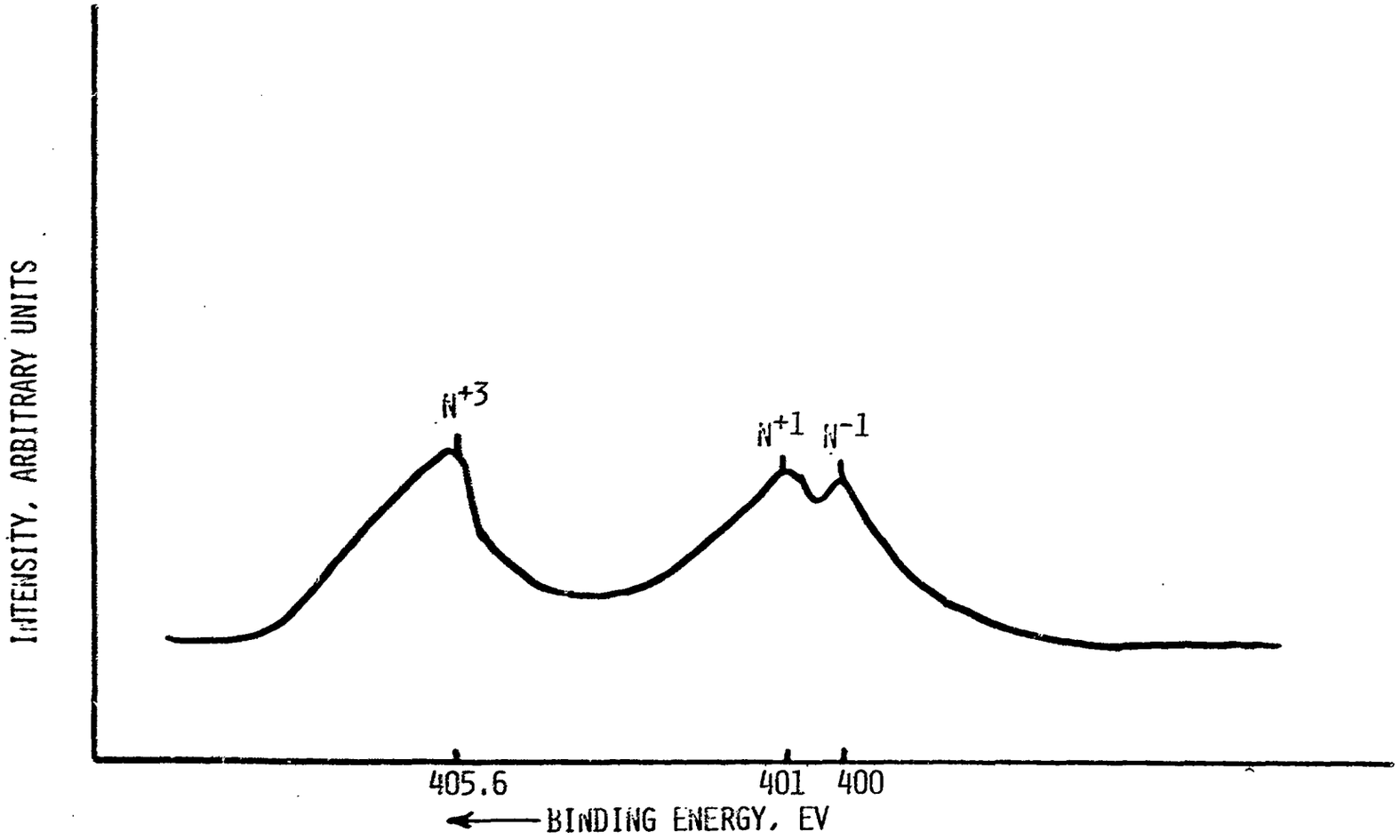

Fig 10 TNT/FS300 adduct after desorption with acetone at 25°C

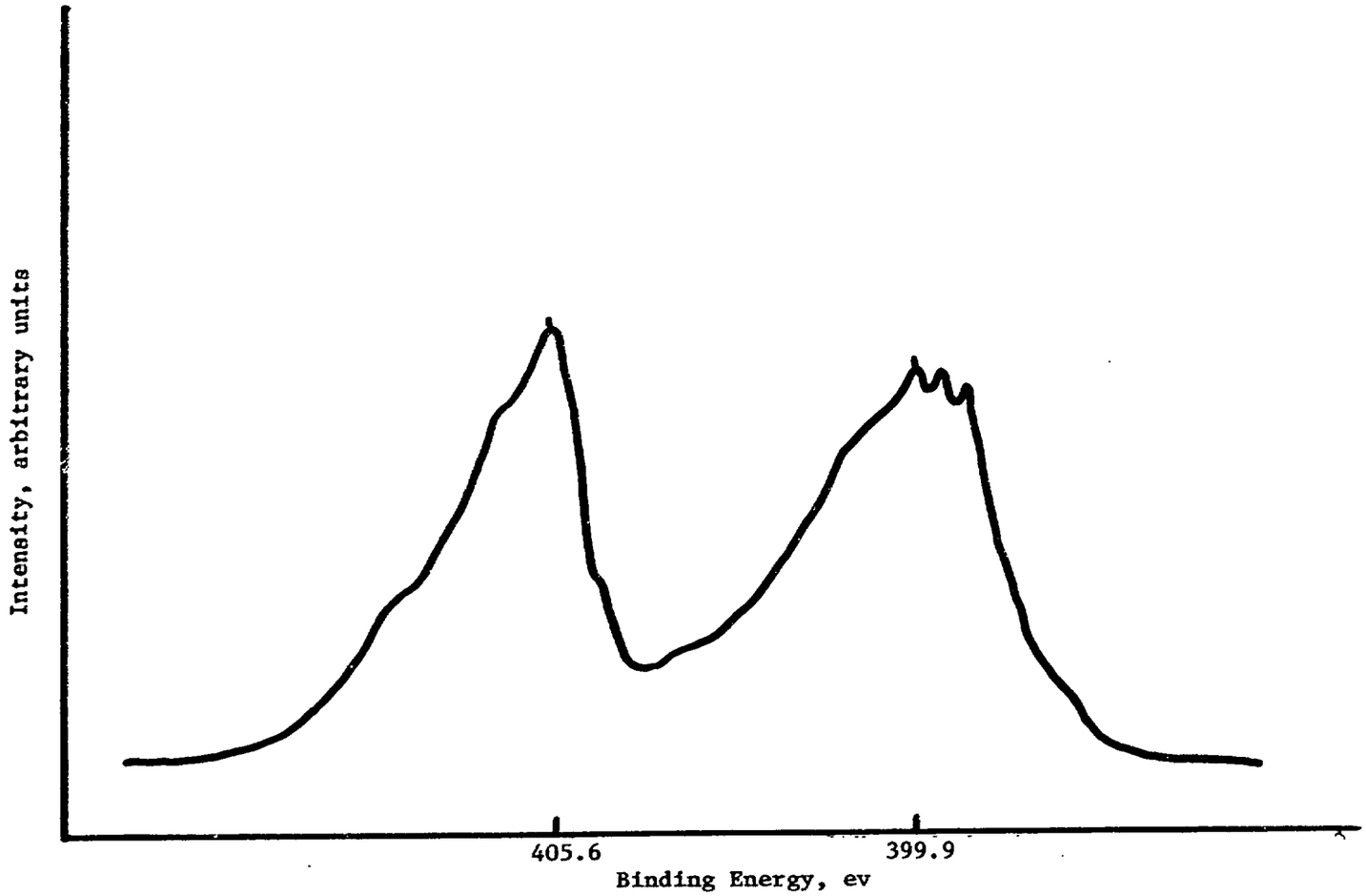

Fig 11 TNT/FS300 adduct after exhaustive acetone soxhlet extraction at 50°C

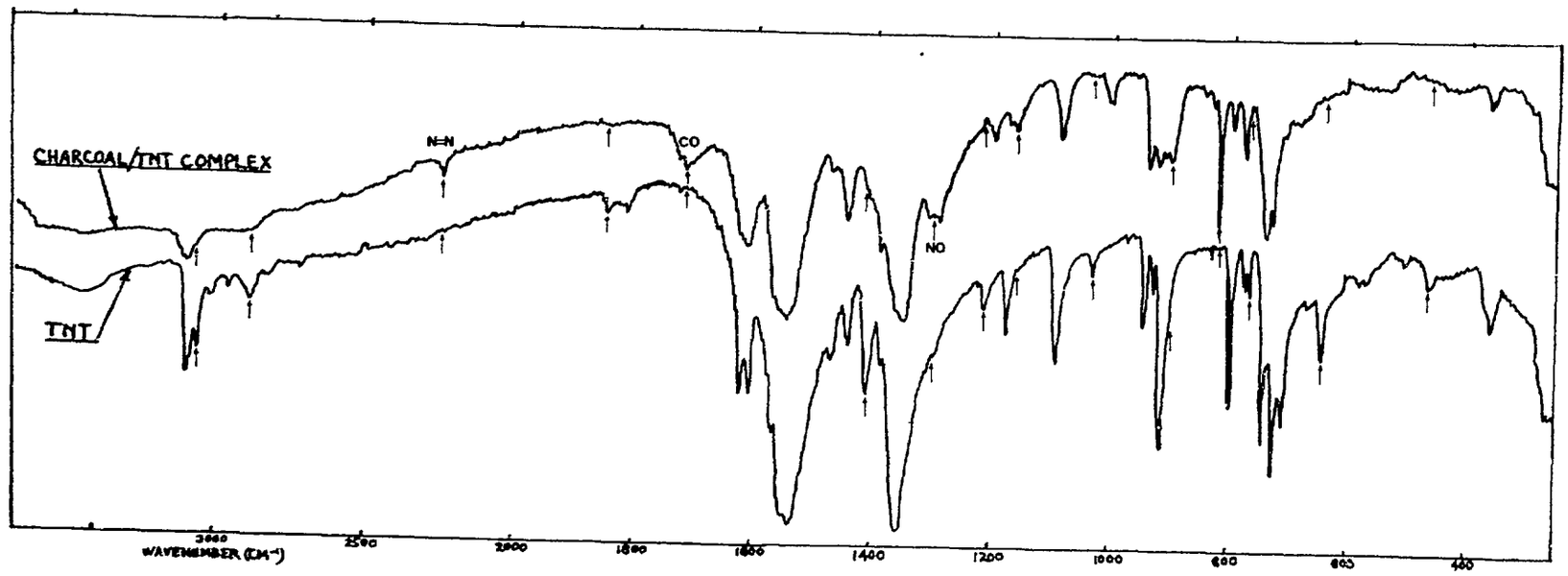

Fig 12 IR spectra of TNT standard and TNT/FS300 complex

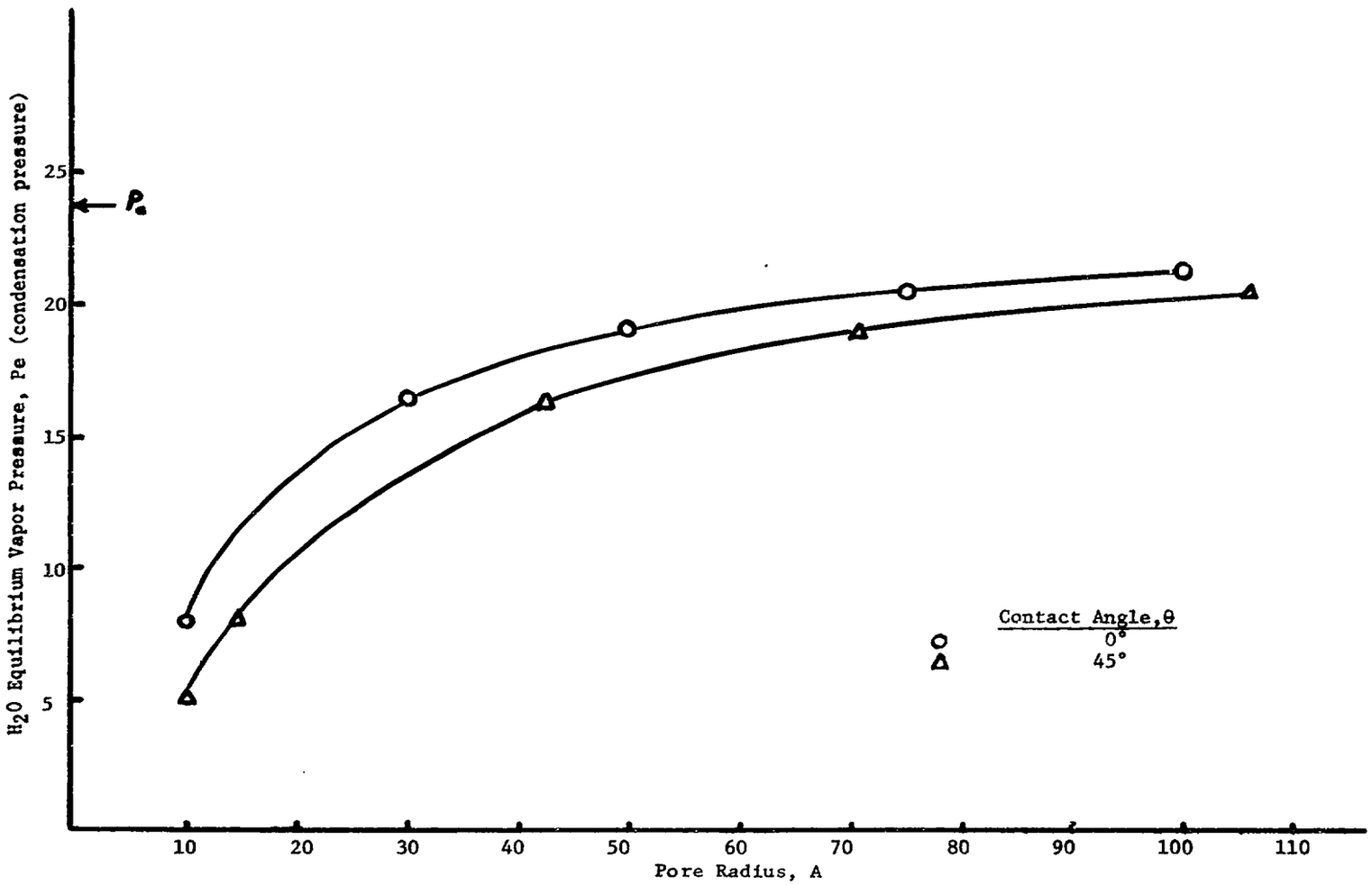

Fig 13 Equilibrium vapor pressure of water in porous structure of FS300 at 25°C

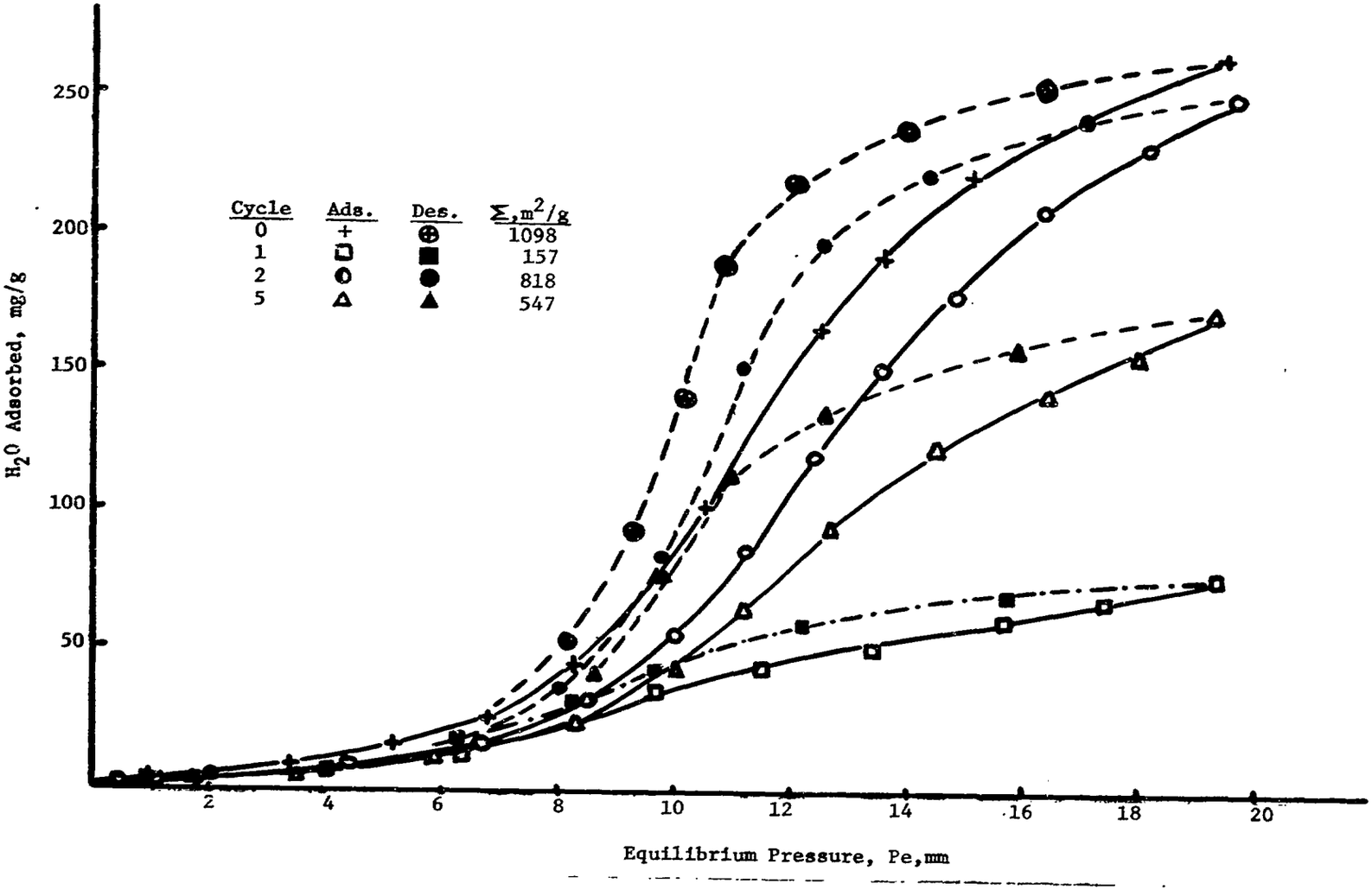

Fig 14 Water adsorption on recycled TNT/FS300 at 25°C

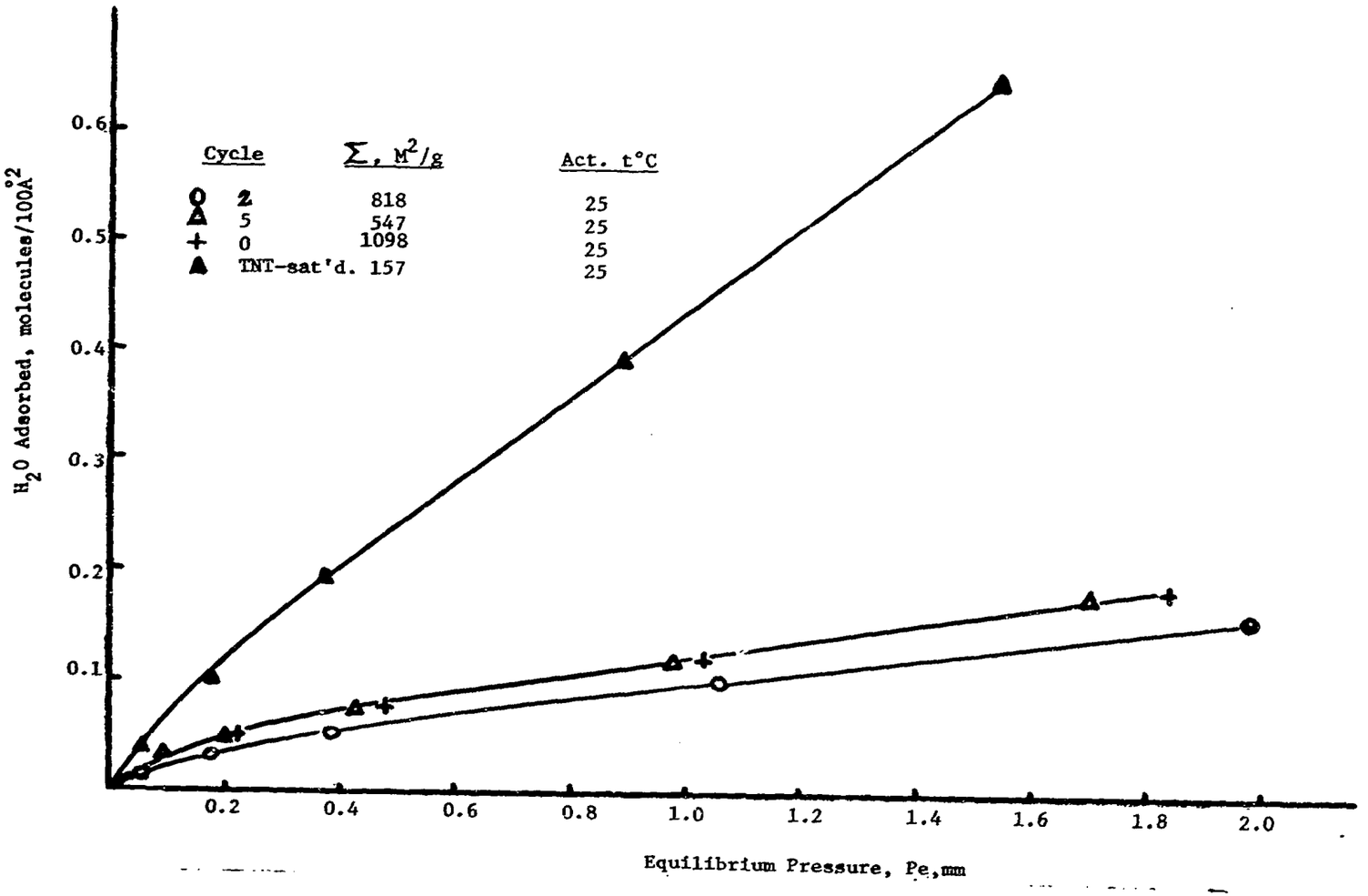

Fig 15 Low pressure region of water adsorption on recycled TNT/FS300 at 25°C

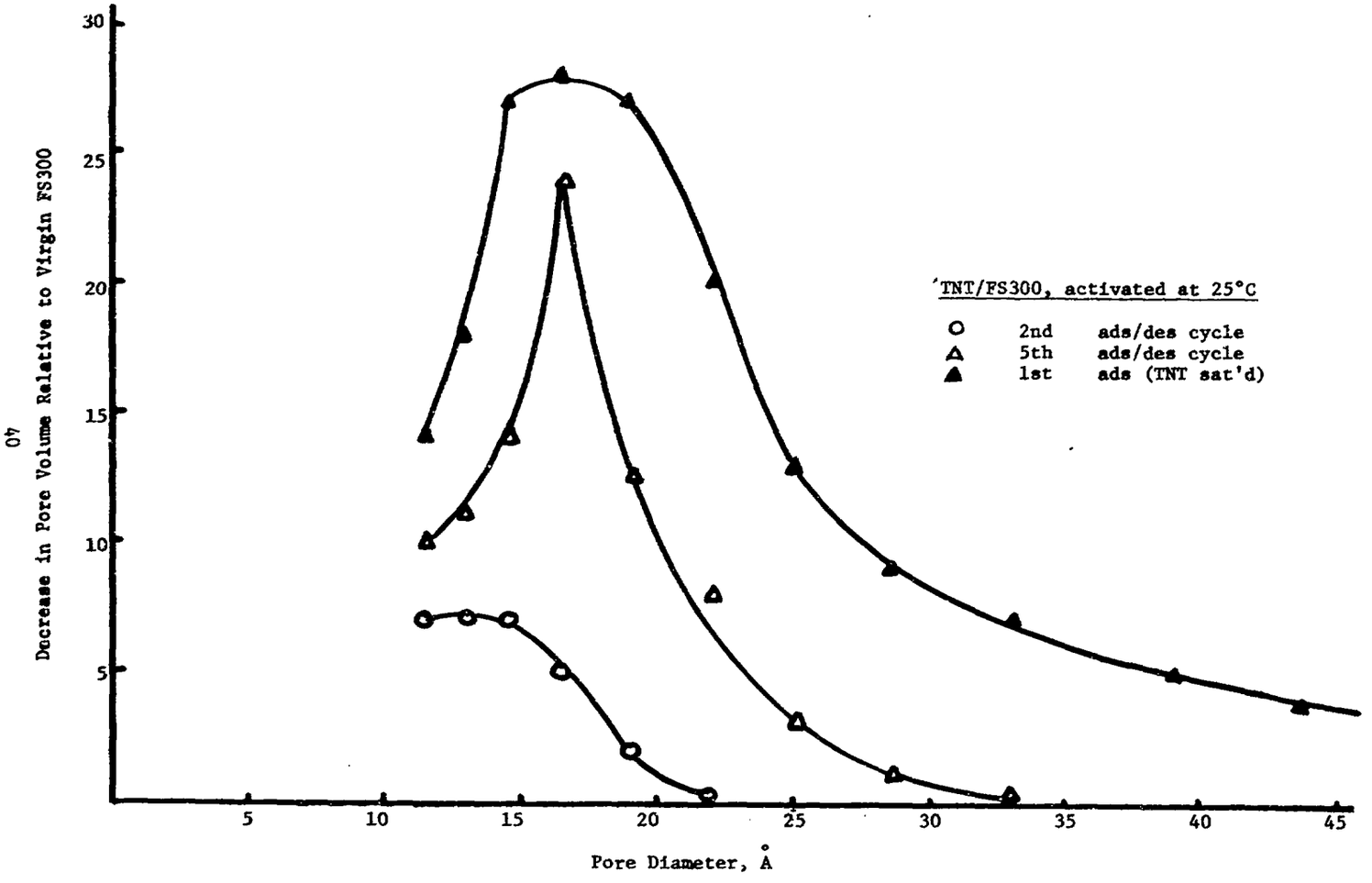

Fig 16 Relative distribution of occluded pore sizes as a function of adsorption/desorption cycles

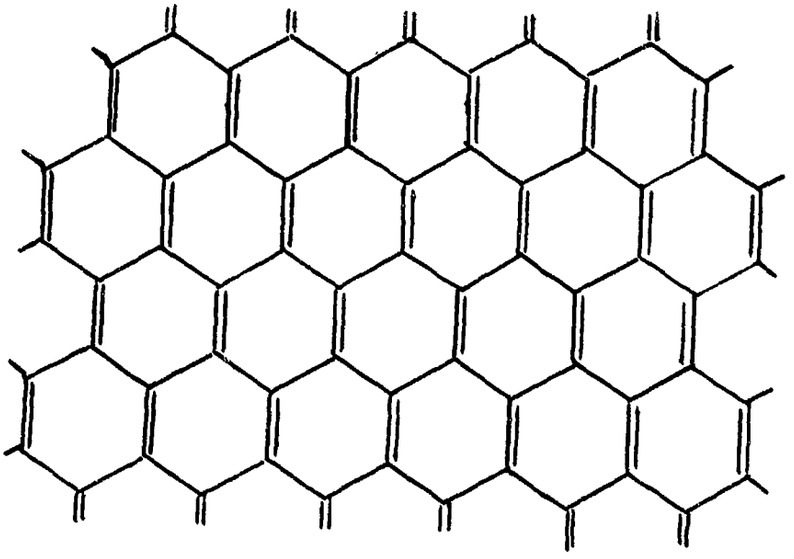

Fig 17 Polynuclear aromatic structure of graphitic surfaces

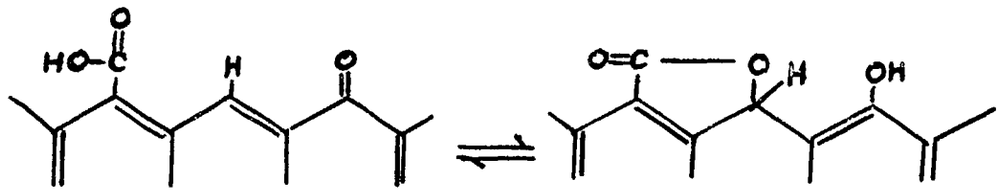

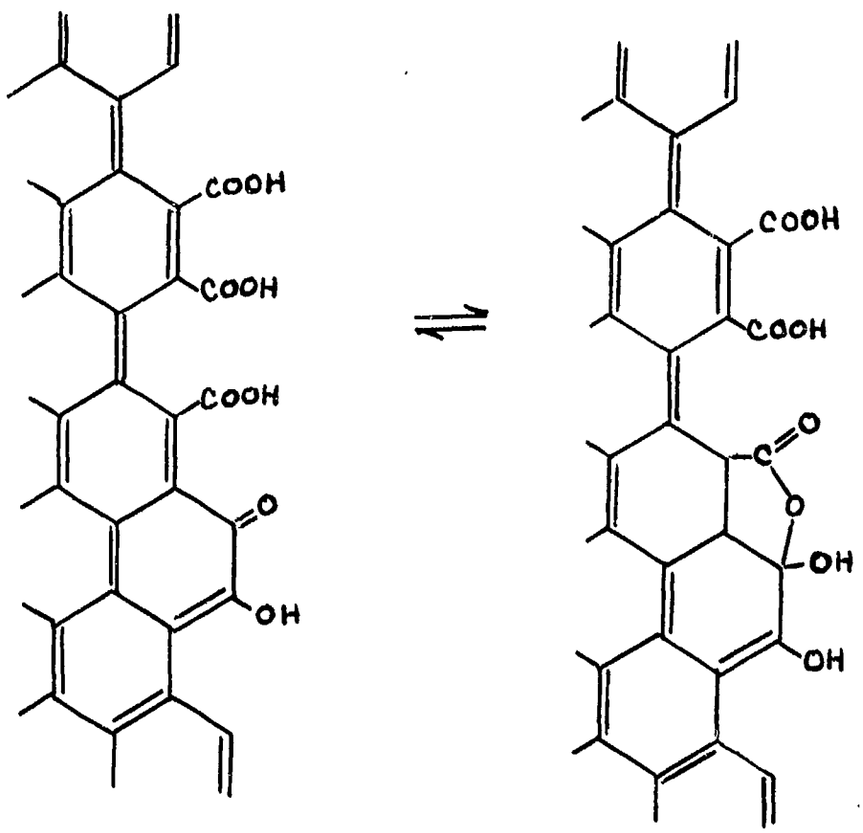

OPEN FORM

LACTONIC FORM

Fig 18 Surface structure models of carbon black according to H.P.Boehm

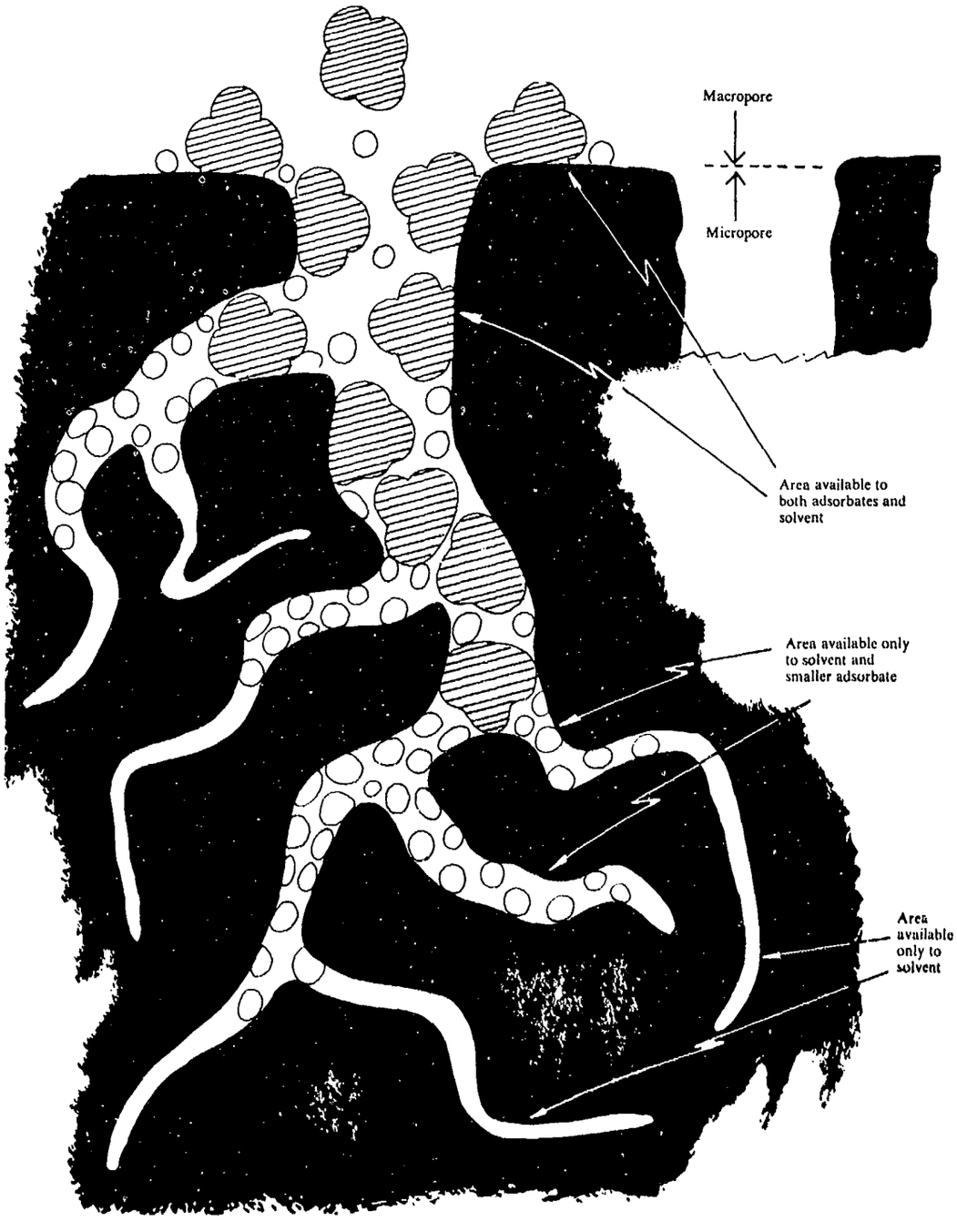

Fig 19 Concept of molecular occlusion of micropores

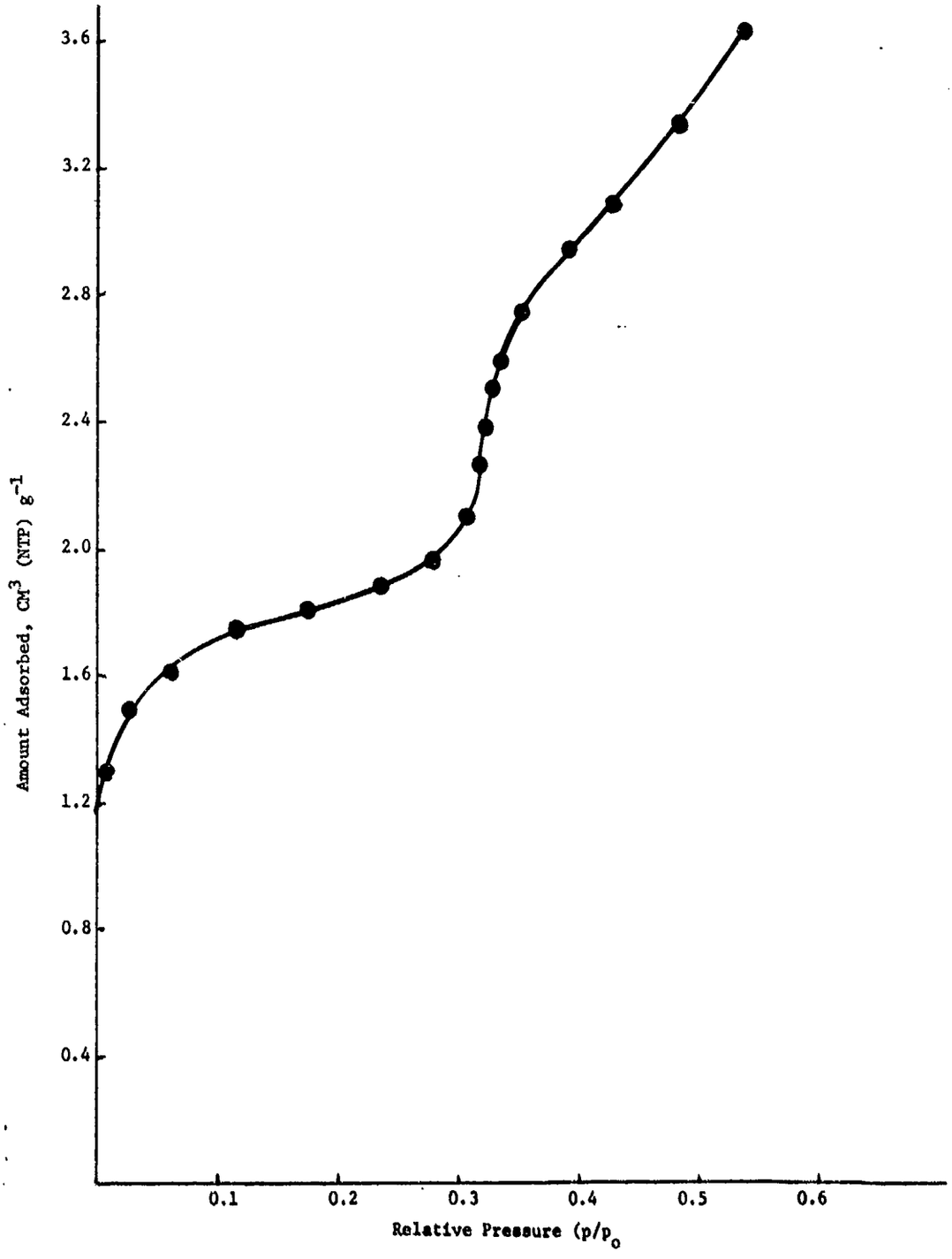

Fig 20 Adsorption of krypton on graphite at -196°C, Σ = 8.3 M^2/g

DISTRIBUTION LIST

	Copy No.
Commander/Director Chemical Systems Laboratory USA ARRADCOM ATTN: A. Hillsmeier D. Renard Aberdeen Proving Ground, MD 21010	 1 2-10
Commander US Army Armament Research and Development Command ATTN: DRDAR-CG, MG B.L. Lewis DRDAR-TD, Dr. R. Weigle DRDAR-TDS, Mr. V. Lindner DRDAR-LC, COL P.B. Kenyon DRDAR-LCM, Mr. L. Saffien DRDAR-LCE, Mr. T.C. Castorina DRDAR-TSS Dover, NJ 07801	 11 12 13 14 15 16-40 41-45
Director Ballistic Research Laboratory USA ARRADCOM ATTN: Technical Library Aberdeen Proving Ground, MD 21010	 46
Commander Radford Army Ammunition Plant ATTN: Dr. W.T. Bolleter Hercules, Inc. Radford, VA 24141	 47
Commander Badger Army Ammunition Plant Baraboo, WI 53913	48
Commander Indiana Army Ammunition Plant Charlestown, IN 47111	49
Commander Holston Army Ammunition Plant Kingsport, TN 37660	50

Commander
Lone Star Army Ammunition Plant
ATTN: Technical Library
Texarkana, TX 75501 — 51

Commander
Milan Army Ammunition Plant
Milan, TN 38358 — 52

Commander
Tooele Army Ammunition Plant
Tooele, UT 84074 — 53

Commander
Iowa Army Ammunition Plant
Silas Mason, Mason & Hanger, Inc.
ATTN: Technical Library
Middletown, IA 52638 — 54

Commander
Joliet Army Ammunition Plant
Joliet, IL 60436 — 55

Commander
Longhorn Army Ammunition Plant
Marshall, TX, 75670 — 56

Defense Documentation Center
Cameron Station
Alexandria, VA 22314 — 57-68

Commander
Louisiana Army Ammunition Plant
Shreveport, LA 71130 — 69

Commander
Newport Army Ammunition Plant
Newport, IN 47966 — 70

Commander
Volunteer Army Ammunition P.
Chattanooga, TN 3740[illegible] — 71

Commander
Kansas Army Ammunition Plant
Parsons, KS 67357 — 72

Commander
US Army Research Office
ATTN: Dr. G. Wyman 73
Box CM, Duke Station
Durham, NC 27706

Commander
Naval Surface Weapons Center
White Oak Laboratory
ATTN: Technical Library 74
Dr. J. Hoffsommer 75
White Oak, Silver Spring, MD 20910

Director
DARCOM Field Safety Activity
ATTN: DRXOS-ES 76
Charlestown, IN 47111

Commander
US Army Training & Doctrine Command
ATTN: ATEN-ME 77
Ft. Monroe, VA 23651

Commander
US Naval Sea Systems Command
ATTN: SEA-0332, Dr. A.B. Amstar 78
Washington, DC 20362

Lawrence Livermore Laboratory
ATTN: Technical Library 79
P.O. Box 808
Livermore, CA 94550

Commander
Fort Detrick
US Army Medical Bioengineering
R&D Laboratory
ATTN: Dr. D.H. Rosenblatt 80
Frederick, MD 21701